3D-NMR Studies of B-Centered *n*-ad Structures in Poly(ethylene-*co*-^{13}C-*n*-butyl acrylate-*co*-carbon monoxide)

Masud Monwar,† Sangrama K. Sahoo,† Elizabeth F. McCord,‡ Samuel D. Arthur,‡ David J. Walsh,‡ and Peter L. Rinaldi*,†

Department of Chemistry, The University of Akron, Akron, Ohio 44325-3601, and Dupont Experimental Station, E. I. DuPont De Nemours and Co., Bldg 328, Rm 133, Route 141 and Powder Mill Rd, Wilmington, Delaware 19880-328

Received December 1, 2005; Revised Manuscript Received February 15, 2006

ABSTRACT: This paper presents the first application of a suite of three-dimensional (3D) NMR techniques for the characterization of complex microstructures in hydrocarbon-based terpolymers. The 3D-NMR experiments are used to disperse and assign the ^1H and ^{13}C resonances of ^{13}C-labeled poly(ethylene-*co*-*1,2,3*-$^{13}C_3$-*n*-butyl acrylate-*co*-carbon monoxide). The one-dimensional (1D) and two-dimensional 2D-NMR spectra of the complex mixture of structures in this polymer are far too complex to interpret. Selective ^{13}C-labeling of all or one carbon in a monomer and use of shaped pulses (which treat the resonances from the labeled ^{13}C as if they were from a third NMR active nucleus) along with 3D-NMR is a solution to this complex problem as it greatly simplifies the spectra by dispersing the resonances into a third dimension and provides atomic connectivity information among three different nuclei. This paper represents the first demonstration of new 3D-NMR methodology for determining structures and resonance assignments of complex hydrocarbon-based structures and mixtures.

Introduction

Nuclear magnetic resonance (NMR) spectroscopy is a very sensitive method for determining the microstructure, monomer sequence, and stereosequence distributions of synthetic polymers. One-dimensional (1D) NMR, especially ^{13}C NMR, has been used for decades to analyze polymer microstructures as it generally gives well-resolved narrow lines from unique structures. The sensitivity of ^{13}C chemical shifts to structural differences in polymer repeat unit sequences of lengths from two to as many as seven (in some cases resonances can be resolved from sequences that differ up to five monomer units away) form the basis of its success as an analytical tool. The advent of higher field spectrometers made it possible to observe resolved lines from longer configurational sequences in the spectra of a number of systems. Quantitative determination of the microstructures becomes possible because, unlike most forms of spectroscopy which require calibrations, a one-to-one relationship exists between intensity and number structures for all resonances in the NMR spectrum. The determination of polymer stereosequence distributions, comonomer sequence distributions, average sequence lengths, structure and distributions of short chain branches, and analyses of end groups become possible from innovative applications of ^{13}C NMR.[1]

However, successful analyses by NMR techniques require that the lines are assigned to specific sequences/structures in the polymers. Empirical resonance assignment techniques, which were initially used, are based on theoretical chemical shift calculations, comparison of relative intensities of resonances based on reaction probabilities, synthesis of model structures, and statistical methods. These methods, although found to be successful in determining monomer and stereosequence distribution, are often tedious and can introduce significant errors and ambiguity in cases where copolymer analyses are performed on complex spectra.

* Corresponding author. E-mail: peterrinaldi@uakron.edu. Telephone: 330-972-5990. Fax: 330-972-5256.
† The University of Akron.
‡ E. I. DuPont De Nemours and Co.

In such cases, two-dimensional (2D) NMR provides additional dispersion in the second dimension, which helps to resolve overlapping peaks in 1D-NMR.[2] The unique occurrence of peaks at the intersection of two resonance frequencies also yields atomic connectivity information, which provide unambiguous resonance assignments. The use of pulsed field gradient (PFG) and higher field spectrometers has made 2D-NMR a more powerful tool as they efficiently remove the unwanted signals and reduce dynamic range problems. These techniques helped to detect and identify the resonances from minor components of synthetic polymers such as chain ends and short chain branches. Recently, Liu et al.[3,4] and Sahoo et al.[5] have applied high-temperature 1D- and 2D-NMR to obtain unambiguous resonance assignment and tacticity information from ethylene/1-alkene polymers. Combinations of different 2D-NMR techniques, such as heteronuclear single quantum coherence (HSQC) spectroscopy and heteronuclear multiple bond correlation (HMBC) spectroscopy provide unambiguous structure identification and resonance assignments. Combined use of several 2D-NMR experiments has become a routine procedure for characterizing homo- and copolymers. However, very little work has been done on the thorough characterization of polymers synthesized from three or more monomers. The spectra of many terpolymers, for example, have peaks that are not well resolved even in 2D-NMR spectra. The mixture of structures resulting from the many possible permutations of three different monomer units in triad sequences makes the spectra from such terpolymers very complex. Unambiguous assignments of individual resonances often become impossible using established methods. The complexity further increases if additional structures are possible from various side reactions[6] and from stereosequence effects.

Three-dimensional (3D) NMR is a more recent technique, which can provide a solution to these problems. Triple-resonance H/C/X 3D-NMR techniques have been used to simplify the spectra of complex polymers by dispersing the $^1H-^{13}C$ correlated 2D-NMR resonances into a third (X-nucleus chemical shift) dimension.[7,8] The spectral simplification and atomic connectivity information obtained from 3D-NMR lead to

10.1021/ma052572f CCC: $33.50
Published on Web 03/21/2006

Table 1. Possible Triad Sequences for PolyEBC

E-centered	B-centered	C-centered
EEE	BBB (3)	CCC
EEB/BEE	EBB/BBE (2)	ECC/CCE
BEC	EBE	ECE
CEB	CBB (2)	BCC
CEE/EEC	BBC (2)	CCB
CEC	CBC	BCB (2)
	EBC	ECB
	CBE	BCE

structural identification and unambiguous resonance assignments. These techniques have been applied to study the structures and stereosequence distributions of a variety of fluoropolymers,[9−13] to identify resonances from the chain ends formed by diphenylphosphinyl radical initiated styrene polymerization[14] and tri-*n*-butyltin-capped polybutadiene,[15] and to characterize the structures and tacticities of polysilanes[16] and polycarbosilanes.[17] All of these applications are based on the presence of a heteroatom (X) such as ^{31}P, ^{19}F, ^{29}Si, or ^{119}Sn in the polymer. Unfortunately, most of the synthetic polymers of research and commercial significance are hydrocarbon-based and lack a third NMR active nucleus; hence, HCX 3D-NMR methods are not applicable in such systems.

In this paper, the application of a recently described suite of multidimensional NMR experiments[18] for characterizing hydrocarbon-based polymer structures is described. These methods involve the use of selective ^{13}C-labeling of the polymer and selective excitation[19] of the resonances from the labeled site (as if they were from a third NMR-active X-nucleus) to produce greatly simplified 3D-NMR spectra. Application of the methodology, analogous to that used for studying protein structures, is illustrated for studying polymers using a sample of ^{13}C-labeled poly(ethylene-*co*-1,2,3-$^{13}C_3$-*n*-butyl acrylate-*co*-carbon monoxide) (polyEB*C) prepared from 1,2,3-$^{13}C_3$-*n*-butyl acrylate ($^{13}CH_2{=}{}^{13}CH{-}{}^{13}CO_2{-}n\text{-}C_4H_9$). The 1D- and 2D-NMR spectra of this terpolymer are very complex because of the large number of possible *n*-ads produced by both monomer- and stereo-sequence effects as well as the presence of branching structures produced by backbiting reactions.[6]

This polymer is composed of three different monomer units; the permutations of triads are listed in Table 1. If polymerization is assumed to occur solely in a head-to-tail manner, up to 27 unique triad monomer sequences are possible.[20] Additionally, some of the triad monomer sequences have two or more stereosequences, since B units form stereogenic centers in the polymer backbone and two adjoining B units give rise to *m* and *r* dyad structures. Although there are 33 nonidentical structural permutations, some of these triads are not likely for various reasons such as low reaction probability due to concentration, steric, and electronic effects. The complexity of the mixture is further increased because of the formation of additional structures from backbiting reactions[6] and chain-end structures. The enormous variety of structures in the mixture produces numerous overlapping peaks even in the 2D-NMR spectra even at 750 MHz. Since the structures in this mixture are part of the same polymer chain, separation and analysis of individual components is not an option. Wyzgoski et al.[21] studied unlabeled polyEBC in attempts to solve the complex problem of assigning the resonances of the terpolymer with the help of 1D-NMR, DEPT, HMQC, HSQC, and HMBC 2D-NMR spectra. They were only partially successful at assigning resonances arising from a number of triad structures and were able to detect some of the cross-peaks consistent with the presence of branching and chain-end structures. Monwar et al.[22] used ^{1}H-detected ^{1}H−^{13}C correlated 2D-NMR of poly(ethylene-*co*-2-^{13}C-*n*-butyl acrylate-*co*-carbon monoxide) obtained from 2-^{13}C-*n*-butyl acrylate (polyEB*^{2}C) and poly(ethylene-*co*-1-^{13}C-*n*-butyl acrylate-*co*-carbon monoxide) obtained from 1-^{13}C-*n*-butyl acrylate (polyEB*^{1}C) to selectively detect and assign the resonances of B-centered pentads in poly(EBC). By using the selective enhancement and spectral simplification provided by selective labeling, they were successful in confirming the prior assignments made from NMR studies of unlabeled polymer and were able to detect some new resonances from species present in low concentration. Using a similar strategy, Al-Amri et al.[23] used ^{1}H−^{13}C HMBC 2D-NMR to detect and assign the resonances of C-centered pentads in poly(ethylene-*co*-*n*-butyl acrylate-*co*-^{13}C-carbon monoxide) obtained from ^{13}C-carbon monoxide (polyEBC*). However, spectral complexity still hindered the resolution and assignment of many resonances in their spectra.

Table 2. Compositions of PolyEBC Samples

polymer	B monomer	mol % E	mol % B	mol % C
polyEBC	$CH_2{=}CHCO_2{-}n\text{-}C_4H_9$	66	8	26
polyEB*^{1}C	$CH_2{=}CH^{13}CO_2{-}n\text{-}C_4H_9$	66	4	30
polyEB*^{2}C	$CH_2{=}{}^{13}CHCO_2{-}n\text{-}C_4H_9$	62	7	31
polyEB*C	$^{13}CH_2{=}{}^{13}CH^{13}CO_2{-}n\text{-}C_4H_9$	65	9	26

Triple-resonance 3D-NMR combined with selective ^{13}C-labeling is a solution to this problem as it greatly simplifies the spectra by dispersing the signals into a third dimension and gives the atomic connectivity information among three different nuclei. Incorporation of ^{13}C-labeled *n*-butyl acrylate (B*) monomers enhances B-centered *n*-ad resonances so that resonances from only one-third of the structures are observed, producing further spectral simplification. Here application of 3D-NMR on poly(EB*C) permits selection and identification of resonances for the structures with ^{13}C-labeled B* units.

Experimental Section

Preparation of ^{13}C-Labeled Poly(EBC) Samples for NMR Analysis. Three selectively ^{13}C-labeled polymers were prepared: one from >99% *1*-^{13}*C*-*n*-butyl acrylate ($CH_2{=}CH^{13}CO_2{-}n\text{-}C_4H_9$), the second from >99% 2-^{13}C-*n*-butyl acrylate ($CH_2{=}{}^{13}CHCO_2{-}n\text{-}C_4H_9$) and the third from >99% 1,2,3-$^{13}C_3$-*n*-butyl acrylate-($^{13}CH_2{=}{}^{13}CH^{13}CO_2{-}n\text{-}C_4H_9$). The resulting polymers are designated by the acronyms polyEB*^{1}C, polyEB*^{2}C, and polyEB*^{1,2,3}C, respectively. The compositions of the polymers are given in Table 2. The preparation and characterization of the polymers used in this study have been previously described.[22] Crystals of 1,4-dichlorobenzene-d_4 were melted, and 20 mg of the polymer was dissolved in 0.7 mL of melt to produce 3% (w/v) polymer solutions. The samples were heated to 120 °C and rotated at 20 rpm in a Kugelrohr oven for 6 h to obtain a uniform dispersion of the polymer in solution and to minimize the formation of air bubbles. Hexamethyldisiloxane (HMDS) was added as an internal chemical shift standard (δ_H = 0.09 ppm; δ_C = 2.0 ppm). All NMR data were collected at 120 °C on a Varian INOVA 750 MHz spectrometer equipped with four rf channels, a Performa-II pulsed field gradient accessory, a Nalorac ^{1}H/^{2}H/^{13}C/^{15}N 5 mm PFG probe designed to operate up to 130 °C, and a ProteinPack software module.

Acquisition of 1D ^{13}C NMR Spectra. The 1D ^{13}C NMR spectra were obtained with a 10 mm broadband (^{15}N−^{31}P) probe, with an 8.5 μs (90°) pulse, 43 kHz spectral width, 1.28 s acquisition time, and 2.0 s relaxation delay. The spectra were obtained with continuous WALTZ-16 modulated decoupling. The data were zero-filled to 256K and exponentially weighted with a 2 Hz line broadening before Fourier transformation.

Acquisition of HSQC and HMBC 2D-NMR Spectra. The HSQC[24] and HMBC[25] spectra were obtained with 90° pulse widths for ^{1}H and ^{13}C of 10.5 and 15.0 μs, respectively, a 0.7 s relaxation

delay, $\Delta = 1.8$ ms ($1/2J$, based on $^1J_{CH} = 140$ Hz), and a 0.25 s acquisition time (with ^{13}C GARP[26] decoupling). Sixteen transients were averaged for each of 2×2048 increments during t_1 using the States[27] method of phase-sensitive detection. The evolution time was incremented to provide the equivalent of a 13.8 kHz spectral width in the f_1 dimension, and a 5.8 kHz spectral width was used in the f_2 dimension. The PFG pulses were 2.0 and 1.0 ms in duration and had amplitudes of 0.196 and 0.098 T/m, respectively. The experiment time was ca. 17 h. Data were linear predicted in the t_1 dimension to double the original number of data points, zero-filled to an 8K $\times$ 8K matrix, and weighted with a shifted sinebell function before Fourier transformation.

The HMBC spectra were obtained in a similar manner for polymer ^{13}C-labeled in methine carbon (polyEB*^{2}C), except that the acquisition time was 0.50 s and the spectrum was collected with spectral windows of 13 kHz (aliphatic carbon region) and 6.0 kHz in the f_1 and f_2 dimensions, respectively. A fixed delay of 0.08 s allowed the heteronuclear antiphase magnetization from long-range coupling to evolve for multiple-bond correlations.

The ester carbonyl region of the HMBC spectrum from the polymer ^{13}C-labeled in ester carbonyl was collected in a different manner. The hard pulses of the ^{13}C channel in the standard ghmqc pulse sequence from Varian's pulse sequence library were changed to half-Gaussian pulses to improve selectivity. A 162.4 μs pulse was used for ^{13}C, with a spectral window of 4 kHz in both the f_1 and f_2 dimensions. A fixed delay of 0.080 s was used to allow the long-range heteronuclear antiphase magnertization to evolve for multiple-bond correlations.

Acquisition of 3D HC_AC_X NMR Spectrum. The 3D HC_AC_X NMR spectrum was collected using the two-channel versions of the pulse sequence previously described.[28] The phases used were along the x axis unless otherwise specified: $\varphi_1 = x, x, -x, -x$; $\varphi_2 = x, -x$; $\varphi_3 = y, y, y, y, -y, -y, -y, -y$; $\varphi_4 = x$; and receiver $= x, -x, -x, x, -x, x, x, -x$. Quadrature components in t_1 were acquired by further altering φ_1 between increments according to the states-TPPI[29] method; echo/anti = echo selection in the t_2 dimension was accomplished by inverting the gradient g_6 and the phase φ_4.[30] Axial peak displacement in the f_2 dimension was obtained by inverting the phase φ_2 and the receiver on every second increment.[31] The 90° pulses for ^{1}H and ^{13}C were 9.8 and 15 μs, respectively. The spectra were acquired with the following parameters: a relaxation delay of 1.0 s, a delay T of 13.5 ms ($1/2J$, based on $^1J_{CC} = 37$ Hz), a delay Δ of 1.9 ms ($1/4J$, based on $^1J_{CH} = 127$ Hz), a delay τ of 0.2 ms, and a 0.25 s acquisition time (with garp1 decoupling); 32 transients were averaged for each of 2×16 increments during t_1, 2×48 increments during t_2, and 1096 total points in t_3. The amplifier compression factors for the proton and carbon channels were calculated by calibrating the pulse widths at two different power levels, and these factors were used in calculating the appropriate power levels for selective pulses. The carbon transmitter was set at 43.0 ppm, and a shifted laminar pulse was created by using the "make180Ca_CO" macro in Varian's ProteinPack software in order to perform off-resonance selective excitation at an offset corresponding to the difference between the center of the ester carbonyl region and the transmitter (175.0−43.0 ppm). The standard Varian macro for setting up HCACO experiments was modified for the offset difference between aliphatic and carbonyl carbon regions of this polymer, which is different from that typically used in protein NMR studies. The selective 90° ^{13}C pulse was calculated using the formula: $\sqrt{15}/4$ * dfrq * (offset difference between aliphatic and carbonyl regions), where dfrq is the ^{13}C decoupler frequency. The WALTZ-16 decoupling sequence with a $\gamma B_1 = 7.5$ kHz was used during the magnetization transfer from C_A to C_X, t_2 evolution time, and t_1 evolution time periods for ^{1}H spin locking and decoupling. The spectral windows in f_1, f_2, and f_3 were 775, 10065.4, and 3286.2 Hz, respectively. The field gradient pulses gt6 and gt9 used for ^{1}H−^{13}C coherence selection had durations of 1.6 and 0.4 ms and amplitudes of 0.20 T/m, respectively. The strengths and durations of pulsed field gradients (PFG) were g1 = 0.28 T/m and 0.5 ms; g2 = 0.15 T/m and 0.5 ms; g3 = 0.30 T/m and 1.0 ms; g4 = 0.20 T/m and 0.3 ms; g5 = 0.15 T/m and 0.2 ms; g7 = 0.15 T/m and 0.6 ms; g8 = 0.25 T/m and 0.4 ms. The total experiment time was 28 h. The data were processed using Varian's VNMR software using f1coef = "1,0,0,0,0,0,−1,0" and f2coef = "1,0,−1,0,0,−1,0,−1". The data were linear predicted to 4 and 2 times the number of points sampled in the t_1 and t_2 dimensions, respectively, zero-filled to $1024 \times 1024 \times 4096$ total points, and weighted with a shifted sinebell function before Fourier transformation. Copies of the setup macros and two- and three-channel versions of 3D-NMR pulse sequences for control of Varian INOVA spectrometers with ProteinPack software can be obtained by sending an e-mail request to the corresponding author.

Acquisition of the 3D HC_AC_X-^{1}H^{1}H-TOCSY NMR Spectrum. The 3D HC_AC_X-^{1}H^{1}H-TOCSY NMR spectrum was collected with the same parameters described above for the 3D HC_AC_X spectrum, with the exception that a DIPSI-2[32] isotropic mixing sequence for 30 ms with $\gamma B_H = 7$ kHz was used for ^{1}H−^{1}H TOCSY transfer between t_2 and t_3. A higher mixing period for TOCSY transfer resulted in loss of signal intensity, and therefore data with a mixing period longer than 30 ms was not used. The data were linear predicted to 4 and 2 times the number of points sampled in the t_1 and t_2 dimensions, respectively, zero-filled to $1024 \times 1024 \times 4096$ total points, and weighted with a shifted sinebell function before Fourier transformation.

Results and Discussion

Structures and Nomenclature. The spectra of polyEBC terpolymers are very complex even in 2D-NMR because of numerous microstructures arising from different permutations of monomer- and stereo-sequences along the polymer backbone. The possible triad monomer sequences shown in Table 1 are subdivided into three groups depending on the central monomer. The complex problem of obtaining resonance assignments can be simplified by studying one of these groups of triad structures at a time. In this work, the B monomer is selectively labeled in the ester carbonyl position with the immediate goal of identifying the resonances of all the B-centered *n*-ad structures and branching structures arising from backbiting reactions at B units.

The ^{13}C chemical shifts are sensitive to variations in structure at least two monomer units away, i.e., to pentad monomer sequences. If stereochemistry is ignored, there are nine pentad sequences for each of the triads in the middle column of Table 1, i.e., a total of 81 B-centered structures. These pentad monomer sequences (ignoring stereochemistry) are summarized in Table 3 along with their Bernoullian formation probabilities.[33] The detection limit of the experiments is estimated between 0.01 and 0.05% so that species (mostly pentads containing 3 or more B units) representing less than ca. 0.01% of the mixture or lower are unlikely to be detected. Species in the 0.01−0.05% range might not be detected depending upon (1) their symmetry and (2) how the reactivity ratios determining their formation deviate from random statistics. In the former case (1), for example, the symmetry of EEBEE pentads is high so the methylene protons on either side of the central CH_{EBE} will contribute to the same resonances; its signals will be more intense because two protons/structure units contribute to many of its resonances. However, a CB**B**BE pentad resonances will be much weaker and difficult to detect; it lacks symmetry because the component CB**B** and **B**BE triads are not the same; and there are four nonequivalent stereoisomers of this pentad. Therefore, four sets of resonances are expected for CBBBE pentads. In the latter case (2), for example, it is known that C will not add to C-terminated radical chain ends, so pentads containing CC dyads in Table 3 (entries with a single slash) will not be detected. This still leaves ~40 pentads. Although the concentrations of many of these (e.g., species containing BC dyads) will be lower than predicted by

Table 3. Possible Pentad Monomer Sequences for PolyEBC[a]

EBE	% probability	EBB	% probability	BBE	% probability
EEBEE	1.607	EEBBE	0.222	EBBEE	0.222
EEBEB	0.222	EEBBB	0.031	EBBEB	0.031
BEBEE	0.222	BEBBE	0.031	BBBEE	0.031
BEBEB	0.031	BEBBB	0.004	BBBEB	0.004
CEBEC	0.257	CEBBC	0.036	CBBEC	0.036
CEBEE	0.643	CEBBE	0.089	CBBEE	0.089
EEBEC	0.643	EEBBC	0.089	EBBEC	0.089
BEBEC	0.089	BEBBC	0.012	BBBEC	0.012
CEBEB	0.089	CEBBB	0.012	CBBEB	0.012

BBB	% probability	CBE	% probability	EBC	% probability
EBBBE	0.031	ECBEE	0.643	EEBCE	0.643
EBBBB	0.004	ECBEB	0.089	EEBCB	0.089
BBBBE	0.004	BCBEE	0.089	BEBCE	0.089
BBBBB	0.001	BCBEB	0.012	BEBCB	0.012
CBBBC	0.005	CCBEC	0.103	CEBCC	0.103
CBBBE	0.012	CCBEE	0.257	CEBCE	0.257
EBBBC	0.012	ECBEC	0.257	EEBCC	0.257
BBBBC	0.002	BCBEE	0.036	BEBCC	0.036
CBBBB	0.002	CCBEB	0.036	CEBCB	0.036

CBB	% probability	BBC	% probability	CBC	% probability
ECBBE	0.089	EBBCE	0.089	ECBCE	0.257
ECBBB	0.012	EBBCB	0.012	ECBCB	0.036
BCBBE	0.012	BBBCE	0.012	BCBCE	0.036
BCBBB	0.002	BBBCB	0.002	BCBCB	0.005
CCBBC	0.014	CBBCC	0.014	CCBCC	
CCBBE	0.036	CBBCE	0.036	CCBCE	0.103
ECBBC	0.036	EBBCC	0.036	ECBCC	
BCBBC	0.005	BBBCC	0.005	BCBCC	
CCBBB	0.005	CBBCB	0.005	CCBCB	0.014

[a] Assumes E:B:C ratio of 65:9:26 determined for polyEB*C.

Bernoullian statistics and will not be detected, additional species will be detected due to permutations of stereochemistry in the middle triads when they contain 2 or more B units. Overall, ca. 30−50 detectable B-centered pentads are expected in the mixture.

In this paper, the nomenclature proposed by Wyzgoski et al.[21] is used to identify atoms in the polymer structure. For completeness and clarity, this nomenclature is briefly described here for the structures relevant to this paper. Since the spectra from the terpolymer samples contain resonances characteristic of long sequences of ethylene monomer units, the general structure for polyethylene is shown at the top of Scheme 1 (**1**). The carbons in this structure are labeled on the basis of nomenclature first defined by Carman[34] and modified by Dorman[35] and Randall.[1] Methylene carbons along the backbone are identified by a pair of Greek letters to indicate the distances to the branches in either direction. Carbons in the side chains are designated by $i\mathrm{B}_n$, where "*i*" indicates the position in the branch starting with the methyl in position 1 and the subscript "*n*" denotes the length of the branch.

The terpolymer samples also contain structures resulting from the addition reactions of C and B units. Wyzgoski et al.[21] proposed a system that is an adaptation of the nomenclature commonly used with polyethylenes. The nomenclature for identifying the carbons of the butoxy groups and for those carbons along the polymer backbone of EBE triads is shown by **2** in Scheme 1. Methine carbons are labeled according to current convention; for example, the methine carbon of the EBE triad is designated as $\mathrm{CH}_{\mathrm{EBE}}$, where the subscript denotes the triad sequence in which the methine is centered. As with ethylene/α-olefin copolymers the backbone methylene groups

Scheme 1. Structures and Nomenclature for Polyethylene (1) and Poly(ethylene-*co*-*n*-butyl acrylate-*co*-carbon monoxide) Structures 2−6

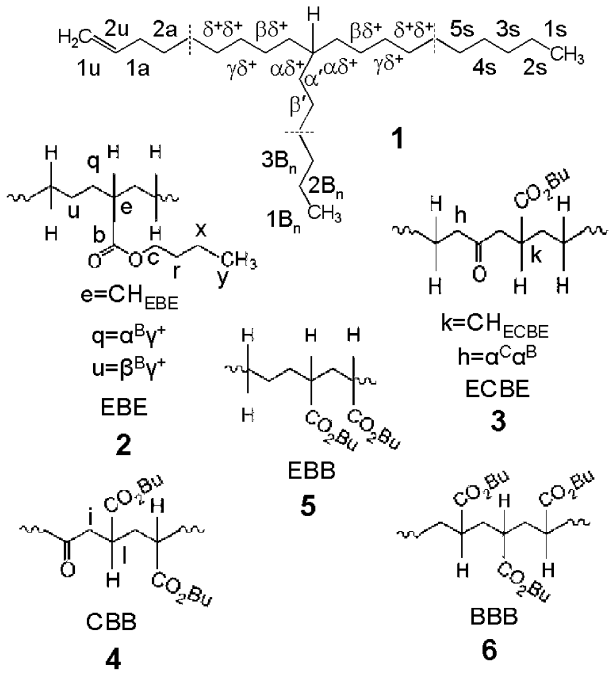

are designated by a pair of Greek letters to indicate the distance from the branches in either direction along the chain. The nature of the branch in ethylene/α-olefin copolymers can be assumed on the basis of the comonomer used (e.g., in ethylene/1-butene copolymers, ethyl branches are formed from 1-butene comonomer). However, in polyEBC, both the nature of the branch and the number of bonds to it must be identified. The type of branch is specified by a superscript B for a butyl acrylate monomer unit and by superscript C for a "branch"[36] formed by the ketone carbonyl. As in the currently used nomenclature for polyethylenes, when the number of methylenes separating a carbon from a branch is greater than a certain number of bonds, a superscripted + is used. Examples of this nomenclature system for identifying B-containing *n*-ads in polyEBC are shown with the structures **2**−**6** in Scheme 1. For example, carbon q of the EBE triad (Scheme 1, **2**) is labeled as $\alpha^{\mathrm{B}}\gamma^{+}$, to indicate this carbon is α to the branch formed by a butyl acrylate monomer unit and that a branch is in the γ position or further along the polymer backbone in the opposite direction.

In this paper, the unlabeled polymer is given the acronym polyEBC, while the polymers ^{13}C-labeled in ester-carbonyl carbon (from *1*-^{13}*C*-*n*-butyl acrylate), methine carbon (from *2*-^{13}*C*-*n*-butyl acrylate), and uniformly labeled in all the acrylate positions of *n*-butyl acrylate (from 1,2,3-$^{13}C_3$-*n*-butyl acrylate) are designated by polyEB*1C, polyEB*^{2}C, and polyEB*C, respectively.

1D-NMR. Figure 1 shows the 1D ^{1}H NMR spectra of the ^{13}C-labeled polyEB*C (Figure 1a), polyEB*^{2}C (Figure 1b), polyEB*^{1}C (Figure 1c), and unlabeled polyEBC (Figure 1d). The ^{1}H NMR spectra are almost identical and contain groups of highly overlapping peaks, making assignments of most resonances almost impossible. The region of interest is from 2 to 3.0 ppm where the methine and methylene peaks of protons α and β to the carbonyl carbons appear. An important feature of the ^{1}H spectrum of poly EB*C and polyEB*^{2}C is the multiplet appearing near $\delta_{\mathrm{H}} = 3.5$ ppm. This has previously been attributed to a B methine α to two carbonyl carbons in a BC dyad ($\mathrm{CH}_{\mathrm{XBC}}$).[22] While it is observed in the spectrum of the

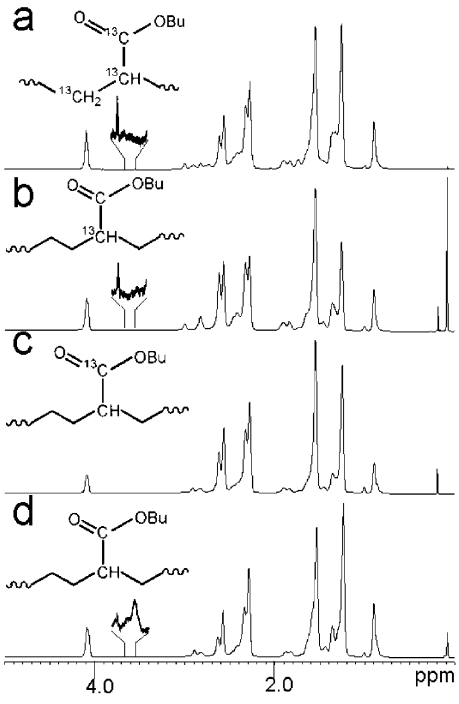

Figure 1. 750 MHz ^{1}H NMR spectra of poly(ethylene-*co*-*n*-butyl acrylate-*co*-carbon monoxide: (a) poly EB*C, (b) polyEB*^{2}C, (c) polyEB*^{1}C, and (d) polyEBC.

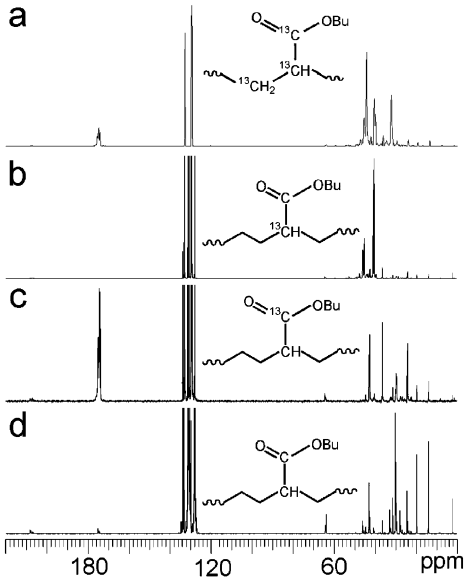

Figure 2. 188 MHz ^{13}C NMR spectra of (a) polyEB*C, (b) polyEB*^{2}C, (c) polyEB*^{1}C, and (d) polyEBC.

unlabeled polymer, it is not detected in the spectra of the labeled polymer. This is possibly because of the different preparation methods used to obtain the labeled polymers or because the signal is weaker due to coupling with ^{13}C from the labeled positions.

Figure 2 shows the ^{13}C NMR spectra of the polyEB*C (Figure 2a), polyEB*^{2}C (Figure 2b), polyEB*^{1}C (Figure 2c), and polyEBC (Figure 2d). All of the spectra are almost identical with the exception of enhancement of ester-carbonyl peaks (~175 ppm) and methine peaks (39−41 and 44−46 ppm) in the spectra of polyEB*^{1}C and polyEB*^{2}C from >99% ^{13}C-labeling of the ester-carbonyl and methine carbons of B units, respectively. In addition to the enhancement of these resonances the uniformly labeled polymer shows additional enhancement of methylene carbon of B unit at ~32 ppm.

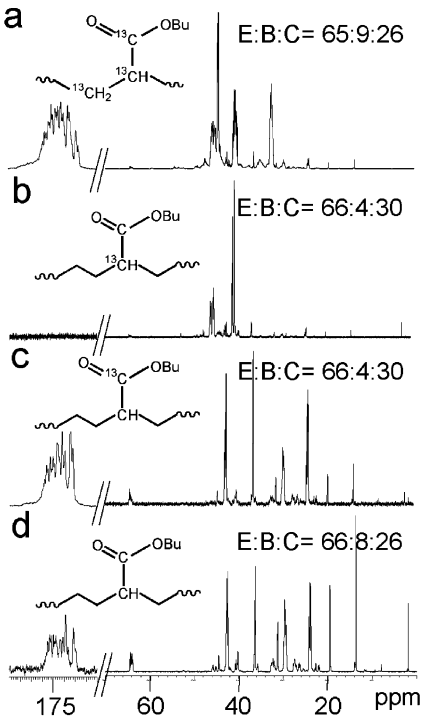

Figure 3. Expansions of the aliphatic and ester-carbonyl regions from the 188 MHz ^{13}C NMR spectra of (a) polyEB*C, (b) polyEB*^{2}C, (c) polyEB*^{1}C, and (d) polyEBC.

Figure 3 shows expansions of the aliphatic and ester-carbonyl regions from the spectra of polyEB*C (Figure 3a), polyEB*^{2}C (Figure 3b), polyEB*^{1}C (Figure 3c), and polyEBC (Figure 3d). In the ester-carbonyl region, the patterns of resonances are very similar in the spectra of polyEB*C (Figure 3a), polyEB*^{1}C (Figure 3c), and polyEBC (Figure 3d) as these samples have similar monomer compositions. However, the signal-to-noise levels in the spectra of the labeled polymers (Figure 3a,c) are much better as expected from the ca. 100-fold increase in the amount of ^{13}C in the labeled ester-carbonyl carbons. More than two dozen overlapping peaks, arising from ester-carbonyl carbons present in different *n*-ad environments are observed; however, it is not possible to assign these from 1D-NMR spectra alone.

Similarly, in the aliphatic region of the ^{13}C spectrum of polyEB*^{2}C (Figure 3b), the resonances in two regions (40−41 and 45−46 ppm) are enhanced from ^{13}C labeling. These resonances appear as more complex patterns in the spectrum in Figure 3a due to the presence of ^{13}C−^{13}C homonuclear coupling in polymer from uniformly labeled *n*-butyl acrylate. A number of weak intensity peaks appeared in the 39−40, 43−44.5, and 47−49 ppm regions, probably from low occurrence triads, branching structures from rearrangement reactions and chain ends. All these increase the complexity of the spectrum. Unambiguous and complete assignment of these peaks is impossible from 1D spectra, indicating the need for *n*D-NMR techniques that provide better dispersion and atomic connectivity information. Similar enhancements are also observed in the aliphatic region of polyEB*C (Figure 3a), with an additional enhancement of the resonances at δ_C ~32 ppm arising from the ^{13}C-labeled methylene carbon of *n*-butyl acrylate. At the same time, some of the peaks in this region which were seen in the spectrum of the unlabeled polymer (Figure 3d) disappear or decrease in intensity because of the lower concentration of the sample. The use of a lower concentration sample increases the molecular mobility, decreases peak line widths, and thus improves the quality of the spectra.

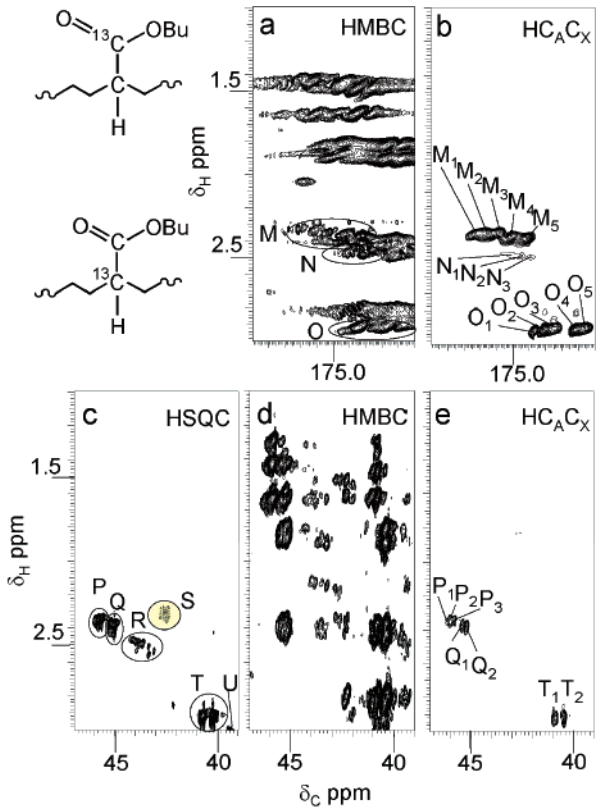

Figure 4. Two-dimensional NMR spectra of labeled polyEBC: (a) ester-carbonyl region from the HMBC 2D-NMR spectrum of polyEB*^{1}C; (b) truncated 3D-NMR spectrum showing one-bond ^{1}H−^{13}C═O (f_1f_3) correlation from ^{1}H/^{13}C/^{13}C═O structure fragments of polyEB*^{1}C; (c) HSQC 2D-NMR spectrum of polyEB*^{2}C; (d) aliphatic region from the HMBC 2D-NMR spectrum of polyEB*^{2}C; (e) truncated 3D-NMR spectrum showing one-bond ^{1}H−^{13}C (f_2f_3) correlation from ^{1}H/^{13}C/^{13}C═O structure fragments in polyEB*C.

2D-NMR. Figure 4 shows expansions of the ester-carbonyl region from the HMBC 2D-NMR spectrum of polyEB*^{1}C (Figure 4a), and the aliphatic regions from HSQC (Figure 4c) and HMBC (Figure 4d) 2D-NMR spectra of polyEB*^{2}C. The HMBC spectra of both polymers show that cross-peaks appear in the same regions of the ^{1}H chemical shift dimensions in these two spectra. However, the HMBC spectrum of polyEB*^{2}C (Figure 4d) also exhibits three-bond correlations to β^B hydrogens (in the δ_H = 1.2−1.4 ppm region) which are not observed in the HMBC spectrum of polyEB*^{1}C (Figure 4a), as the β^B hydrogens are four bonds away from the ^{13}C-labeled carbon atoms in the latter. These spectra provide important atomic connectivity information and lead to unambiguous assignments for a number of resonances. There is also significant overlap in the 2.3−2.5 and 2.8−3.0 ppm regions of the HMBC spectrum of polyEB*^{1}C because of the similar chemical shifts of many different methine and methylene ^{1}H resonances. Here 3D-NMR can provide an additional increase in spectral dispersion to surmount these difficulties.

A cluster of unresolved ester-carbonyl resonances could be detected in δ_C = 174.9−175.4 ppm region of the HMBC spectrum (cross-peaks in area M of Figure 4a) with correlations to CH_{EBE} protons having ^{1}H chemical shift in the 2.3−2.5 region.[22] Three moderately resolved broad cross-peaks were also identified in region O of Figure 4a at δ_C = 174.1−174.7 ppm and in the ^{1}H chemical shift region of 2.8−3.0 ppm; these have been previously assigned to CH_{CBE}. Similarly, in the case of polyEB*^{2}C, resonances in the region of 45−46 and 40−41 ppm of the HSQC spectrum could be assigned with help of the HMBC spectrum, but resonances in the 43.0−44.5 and 39.0−40.0 ppm regions could not be assigned unambiguously because of the severe overlap or missing cross-peaks in the HMBC spectrum.[22]

3D-NMR. The HC$_A$C$_X$ and HC$_A$C$_X$-^{1}H^{1}H-TOCSY pulse sequences used in this work are shown in Figure 5a,b; they work by sequential INEPT[37] transfer steps from ^{1}H to the $^{13}C_{aliphatic}$ atoms (α to carbonyl carbon) and then to ^{13}C═O, using one-bond proton−carbon ($^1J_{CH}$) and carbon−carbon ($^1J_{CC}$) couplings, respectively. The t_1 evolution period is used to encode the carbonyl carbon shifts and to accomplish reverse INEPT transfer of magnetization from ^{13}C═O back to $^{13}C_{aliphatic}$; a constant evolution time $2T$ is used to encode the $^{13}C_{aliphatic}$ chemical shifts in the t_2 evolution time; a reverse INEPT transfer from $^{13}C_{aliphatic}$ to ^{1}H is performed; and antiphase magnetization created during the beginning of the sequence is refocused during the second pair of delays before detection of the protons during the acquisition time t_3. The ^{13}C decoupler offset was shifted from $^{13}C_α$ to ^{13}C═O region, and a shifted laminar pulse was used for selective inversion of $^{13}C_α$ during the ^{13}C═O chemical shift evolution period. A Waltz-16 spin-lock is used to lock the transverse magnetization of $^1H_α$ during the magnetization transfer from $^{13}C_α$ to ^{13}C═O and during t_1 and t_2 evolution periods, so that homonuclear couplings between $^1H_α$ and other protons are removed. The HC$_A$C$_X$-^{1}H^{1}H-TOCSY sequence uses a ^{1}H spin-lock mixing period before data acquisition to distribute the magnetization over protons that are part of the same spin system.

These sequences are patterned after the HCACO sequence used to identify $H_α$−$C_α$−C═O atomic connectivities in the backbone structures of proteins.[38] The sequence in Figure 5a can be viewed as a more general version of the HCACO experiment, since the pulse program has been altered in several ways. (1) It allows adjustment of the polarization transfer delays needed to accommodate the range of $^1J_{CC}$ couplings and multiplicities encountered in general structures. (2) It permits the arbitrary placement of C_A and C_X transmitter offsets, where $^{13}C_A$−$^{13}C_X$ form an AX spin system (rather than the predetermined values needed to excite $H_α$−$C_α$−C═O fragments in a polypeptide backbone). (3) Pulse sequence elements needed to decouple ^{15}N in uniformly labeled proteins are absent.

Figure 4b,e contains plots of the truncated HC$_A$C$_X$ 3D-NMR spectra showing ^{1}H−^{13}C═O (f_1f_3) correlations (Figure 4b) and ^{1}H−$^{13}C_α$ (f_2f_3) correlations (Figure 4e) from the ^{1}H−^{13}C−^{13}C═O structure fragments in the polymer. The truncated 3D spectra are 2D-NMR spectra collected using the same 3D-NMR pulse sequences described above, keeping one of the evolution times fixed. The truncated f_2f_3 3D spectrum, collected with t_1 fixed, then becomes equivalent to an HSQC spectrum showing C−H correlations of directly bonded atoms, but with filtering of all resonances from the spectrum except for those CH_n groups bound to the ^{13}C-labeled carbonyl groups. The truncated 3D-NMR spectra of polyEB*C should be compared with the HSQC spectrum of polyEB*^{2}C and HMBC spectra of polyEB*^{1}C and polyEB*^{2}C as the cross-peak patterns in the HSQC and HMBC spectra of polyEB*C are complicated by one-bond and multiple-bond ^{13}C−^{13}C couplings.

The two truncated 3D-NMR spectra (Figure 4b,e) were collected by fixing t_2 and t_1, respectively, to produce the 2D projections of the f_1f_3 and f_2f_3 planes from the 3D-NMR spectra, respectively. These planes exhibit two-bond **^{1}H**−**$^{13}C_α$**−**^{13}C**═O and one-bond **^{1}H**−**$^{13}C_α$**−^{13}C═O correlations similar to those observed in the HMBC and HSQC 2D-NMR spectra. However, the standard 2D-NMR spectra show all the possible C−H

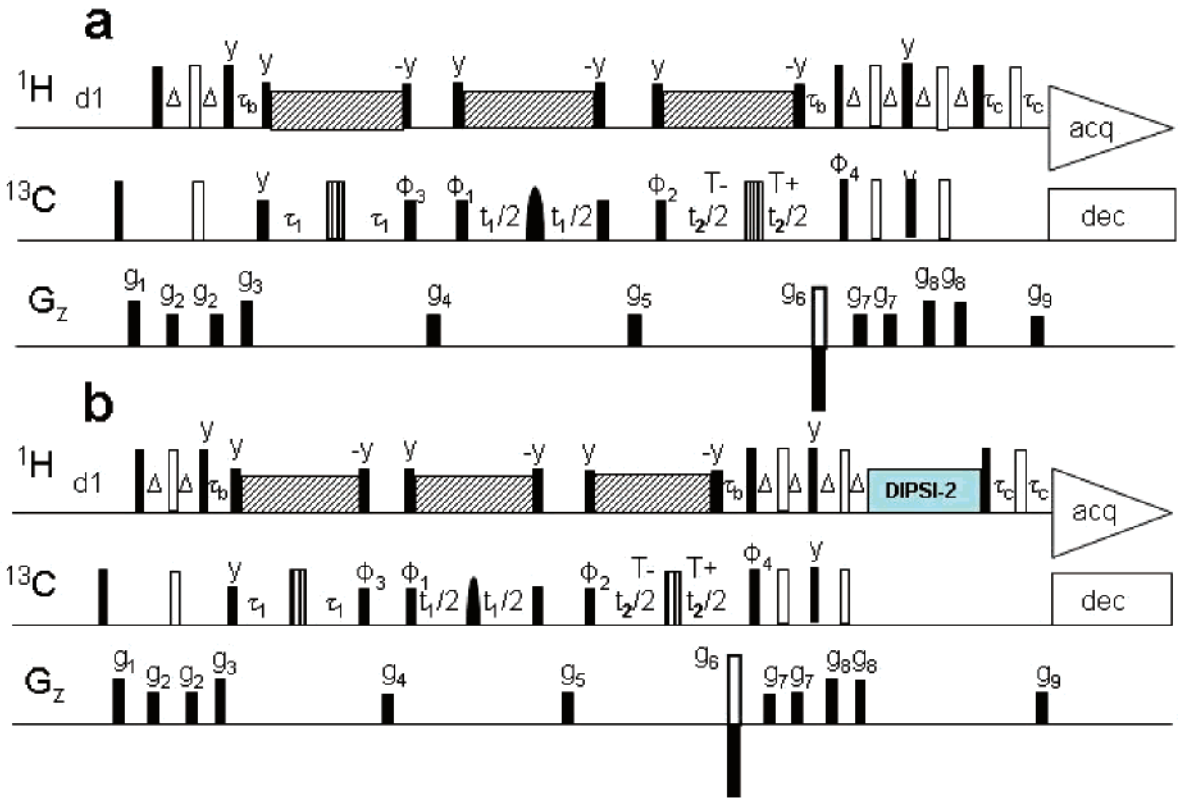

Figure 5. 3D pulse sequences used to collect the 3D-NMR spectra of ^{13}C-labeled polyEB*C: (a) HC_AC_X and (b) HC_AC_X-$^1H^1H$-TOCSY with spin-locking.

correlations, while the truncated 3D-NMR spectra exhibit only those resonances arising from the two bond correlations in $^1H-^{13}C_\alpha-^{13}C{=}O$ structure fragments. The constant evolution period and the selective $^{13}C_\alpha$ inversion pulse in the HC_AC_X pulse sequence effectively remove ^{13}C homonuclear couplings in the indirectly detected f_1 and f_2 dimensions of the truncated 3D-NMR and results in simpler peak patterns compared to HMBC and HSQC spectra, where these couplings are present in the indirectly detected dimensions. For example, compare the standard HMBC spectrum of polyEB*^{1}C in Figure 4a with the truncated 3D-NMR spectrum of polyEB*C in Figure 4b. The complex cross-peak patterns M, N, and O in the standard HMBC spectrum from polyEB*^{1}C (Figure 4a) are greatly simplified by the presence of a single isolated ^{13}C label and the observation of correlations from two bond couplings, so that it is possible to identify distinct cross-peaks (M_1-M_5, N_1-N_3, and O_1-O_5) in these regions of the truncated 3D-NMR spectrum. In fact, many cross-peaks would not even be identifiable in the HMBC spectrum if it were not for their observation in the truncated 3D-NMR spectrum. All other correlations in the 2.3−3.0 ppm region which do not belong to $^1\mathbf{H}-^{13}C_\alpha-^{13}\mathbf{C}{=}O$ structure fragments are filtered from the spectrum.

Similarly, the f_2f_3 truncated 3D-NMR spectrum in Figure 4e, acquired with a single fixed t_1 evolution period, shows direct C−H correlations comparable to those found in a standard HSQC 2D-NMR spectrum. Filtering all the resonances but those of $^1\mathbf{H}-^{13}\mathbf{C}_\alpha-^{13}C{=}O$ structure fragments removes the resonances observed in regions R and S of the HSQC spectrum (Figure 4c) from the truncated 3D-NMR spectrum (Figure 4e).

In the HSQC spectrum (Figure 4c) of polyEB*^{2}C six clusters of cross-peaks are observed (regions P−U). With the exception of the cross-peaks in cluster *S* all of the correlations arise from methine groups (as determined by the phase of the HSQC cross-peaks). Cluster *P* shows two broad overlapped cross-peak clusters centered at $\delta_C = 45.80$ and 45.64 ppm correlated with proton resonances with a ^1H chemical shift of 2.35 ppm. Cluster *Q* also consists of two broad overlapped cross-peaks at $\delta_C =$ 45.26 and 45.05 ppm and correlated with proton resonances at $\delta_H = 2.38$ ppm. Cluster *T* has two broad clusters of cross-peaks at $\delta_C = 40.65$ and 40.25 ppm correlated with ^1H resonances with a chemical shift of 2.92 ppm. Two other broad clusters consisting of four to six highly overlapped low-intensity cross-peaks are observed in the $\delta_C = 44.3-43.5$ ppm and $\delta_H \sim 2.50$ ppm region (cluster *R*) and in the $\delta_C = 39.1-39.6$ ppm and $\delta_H \sim 3.0$ ppm region (cluster *U*).

In the f_2f_3 truncated 3D-NMR spectrum (Figure 4e) which shows $^1H-^{13}C$ correlations of the $^1\mathbf{H}-^{13}\mathbf{C}-^{13}C{=}O$ structure fragments cluster *P* simplifies to three well-resolved cross-peaks at $\delta_C = 46.18$ (P_1), 46.0 (P_2), and 45.80 ppm (P_3), and two well-resolved cross-peaks at $\delta_C = 45.44$ (Q_1) and 45.22 ppm (Q_2) are observed corresponding to cluster Q from the HSQC spectrum. Cluster T from the HSQC spectrum simplifies to two well-resolved cross-peaks in the truncated 3D (f_2f_3) spectrum at $\delta_C = 40.87$ (T_1) and 40.45 ppm (T_2). In each case it is observed that the broad overlapped peaks in the HSQC spectrum are more disperse and well-resolved in the truncated 3D-NMR spectrum. Clusters R and U are not found in the truncated 3D spectrum because of their lower intensity which might appear if more increments would be collected. Cluster S was not found in the truncated 3D spectrum as it is arising from methylene carbons and not associated with the $^1\mathbf{H}-^{13}\mathbf{C}-^{13}C{=}O$ structure fragments. However, the truncated 3D-NMR spectra still lack a second indirectly detected dimension. In a full 3D-NMR spectrum, arrays of data are collected in both of the indirectly detected dimensions, and this additional dimension further disperses the resonances, resulting in additional spectral simplification.

3D-NMR. Analysis of 3D Data and Resonance Assignments. All possible triad monomer sequences are shown in Table 1. Of all the possible sequences, only B-centered *n*-ad sequences listed in the middle column need to be considered here, as the ^{13}C-labeling patterns and 3D pulse sequences used filter the remaining resonances from the spectra. Of these, structures containing BBB sequences need not be considered because of their low formation probabilities (due to low concentration of B in the polymer). This leaves the resonances of EBE, CBE, EBC, BBE, EBB, BBC, and CBB triads to be assigned. In assigning the peaks, it has been considered that proton shifts are primarily sensitive to triad monomer sequences while carbon shifts are sensitive to higher *n*-ads sequences.

In analyzing the planes and assigning the resonances, the following nomenclature has been used in the discussions below. Each pair of f_2f_3 planes in the 3D-HC$_A$C$_X$ and HC$_A$C$_X$-^{1}H^{1}H-TOCSY spectra correspond to a particular B-ester carbonyl shift ($\delta_{C=O}$). The 3D-HC$_A$C$_X$ cross-peaks in the f_2f_3 planes are designated with bold italic letters (***a***, ***b***, ***c***, ..., in Figure 6b−f), each corresponding to an ester carbonyl group to which the methine is attached. These labels also correspond to the resolved ^{13}C ester carbonyl shifts of unique B-ester carbonyl carbons in the 1D ^{13}C NMR spectrum. The planes in the 3D HC$_A$C$_X$ spectrum establish the unique **^{1}H−^{13}C$_\alpha$−^{13}C**═O structure fragment connectivities. They do not provide unequivocal information about remote structure; however, they do help to identify cross-peaks from directly connected H−C−C atoms in the HC$_A$C$_X$-^{1}H^{1}H-TOCSY spectrum. These same **^{1}H−^{13}C$_\alpha$−^{13}C**═O correlations are also seen in the HC$_A$C$_X$-^{1}H^{1}H-TOCSY spectrum and are designated with the same labels. Additionally, TOCSY correlations are observed, dispersed in the ^{1}H (f_3) chemical shift dimension of Figure 6h−l. For example, correlation ***a*** (in Figure 6h) is related to several TOCSY correlations with resonances of protons on adjoining carbons that form a unique mutually H−H homonuclear coupled spin system; these additional H−H TOCSY correlations are designated with the same letter and a numerical subscript (***a$_1$***, ***a$_2$***, ***a$_3$***, ...). The diastereotopic methylene protons are designated with (***a$_1$***/***a$_1$′***, ***a$_2$***/***a$_2$′***, ...).

The HC$_A$C$_X$ and HC$_A$C$_X$-^{1}H^{1}H-TOCSY spectra are interpreted in the following manner. Typically, in the HC$_A$C$_X$ spectrum each pentad gives rise to resolvable **^{1}H−^{13}C$_\alpha$**−^{13}C═O cross-peak in an f_2f_3 plane at the f_1 chemical shift of its carbonyl carbon. If an f_2f_3 plane from the HC$_A$C$_X$-^{1}H^{1}H-TOCSY spectrum is examined at this same f_1 chemical shift, this same **^{1}H−^{13}C$_\alpha$−^{13}C**═O correlation can be observed. This plane also contains the TOCSY peak patterns identifying the resonances of protons on adjoining monomer units which can then be interpreted in a logical and systematic way to identify the monomer units adjoining the central B-unit. Each methine C−H of a B-centered pentad -WX**B**YZ- (where W, X, Y, and Z represent E, C, or B units), will exhibit H−H TOCSY correlations to the α^B and β^B proton resonances of X and Y monomer units in -WX**B** and **B**YZ- triads. The chemical shift of these proton resonances are sensitive to the type of W and Z monomer units, respectively, and show characteristic shifts depending on the specific triad sequence. For example, the ^{13}C resonance of the central methine carbon in EE**B**EC pentad will exhibit correlations to the two sets of ethylene α^B and β^B proton resonances from the EE**B** and **B**EC triads on either side of the central **B** in the pentad unit. Each of these triads will yield a unique and easily identifiable ^{1}H chemical shift pattern. The α^B proton resonances of the E unit in a **B**EC triad will show a significant downfield shift compared to the α^B proton resonance of the central E unit of an EE**B** triad because of the deshielding effect from the C unit carbonyl group. Interpretation of the HC$_A$C$_X$-^{1}H^{1}H-TOCSY spectrum is simply a matter of recognizing the two ^{1}H chemical shift patterns at each of the ^{13}C chemical shifts. For symmetric pentads such as EEBEE, equivalent patterns will be superimposed from the EEB and BEE triads on either side of the center B-unit. The dispersion provided by the combined use of very high field and 3D techniques made it possible to resolve separate patterns for each of the pentads present at detectable concentrations.

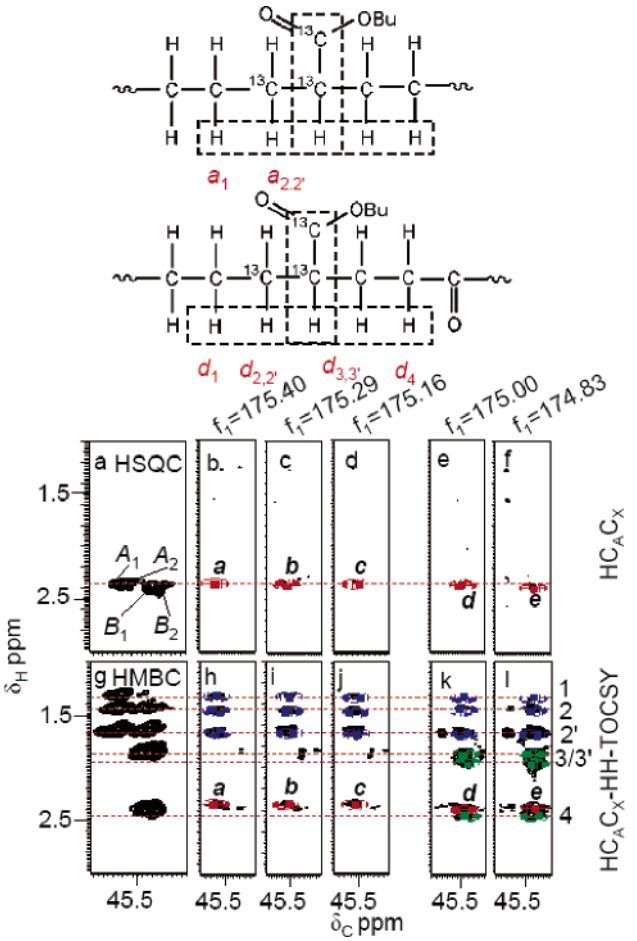

Figure 6. Expansions from the 2D (a and g) and 3D (b−f and h−l) NMR spectra of ^{13}C-labeled poly(EB*C) showing the 44.5−46.5 ppm region: (a) HSQC spectrum of polyEB*^{2}C; (b−f) f_2f_3 planes from the 3D-HC$_A$C$_X$ spectrum of polyEB*C; (g) HMBC spectrum of polyEB*^{2}C; (h−l) f_2f_3 planes from the 3D-HC$_A$C$_X$-^{1}H^{1}H-TOCSY spectrum of polyEB*C and assignment of EEBEE and EEBEC pentads. The f_1 chemical shifts are printed across the tops of the respective planes from the 3D spectra.

EBE-Centered Structures. Figure 6 shows selected f_2f_3 planes (^{13}C$_{aliphatic}$−^{1}H correlations) from the HC$_A$C$_X$ (Figure 6b−f) and HC$_A$C$_X$-^{1}H^{1}H-TOCSY (Figure 6h−l) 3D-NMR spectra, arising from ^{1}H−^{13}C−^{13}C═O structure fragments in EEBEX pentads. The separation between 3D planes is 0.032 ppm in both the f_1 and f_2 dimensions. These are to be compared with the HSQC (Figure 6a) and HMBC (Figure 6g) 2D-NMR spectra of polyEB*^{2}C. The peaks (cluster ***A***$_1$/***A***$_2$) in the HSQC (Figure 6a) are dispersed in the ^{13}C$_{C=O}$ chemical shift dimension of the 3D-NMR spectra, indicating that several peaks arising from higher *n*-ad environments are overlapping and form the clusters of cross-peaks in the 2D-NMR spectra. As the polymers are labeled, ^{13}C−^{13}C coupling could also be responsible for the broadness of the peaks in the 2D-NMR spectra. These overlapped peaks have been resolved into three well-defined cross-

peaks, ***a***, ***b***, and ***c***, in the planes (Figure 6b−d) of the 3D-HC_AC_X spectrum. These sharp peaks result because the 3D pulse sequence used to collect this spectrum selectively excites resonances arising from $^1H-^{13}C-^{13}C{=}O$ structure fragments and effectively removes any $^{13}C-^{13}C$ coupling by appropriate placement of selective ^{13}C inversion pulses and by the use of constant time evolution periods.

In a similar way, the long-range C−H correlations in the HMBC spectrum (Figure 6g) are also dispersed into the $^{13}C_{C=O}$ dimension of the HC_AC_X-$^1H^1H$-TOCSY spectrum (Figure 6h−j). In addition, the cross-peaks in the HMBC spectrum are spread in the ^1H dimension because of homonuclear coupling between $^1H_\alpha$ and other protons and chemical shift dispersion caused by long-range (*n*-ad where $n > 5$) structure variations. The 2D-NMR cross-peaks at positions 2/2′ and 3/3′ ($\delta_H = 1.46/1.66$ and 1.82/1.92 ppm) are seen to form clusters with extensive overlap. These broad overlapped peaks are dispersed and clearly resolved in the HC_AC_X-$^1H^1H$-TOCSY spectrum.

In earlier work,[22] despite the broadness of the cross-peaks ***A₁*** and ***A₂*** in the HSQC spectrum, they were assigned with the aid of the HMBC spectrum. The broad clusters of peaks in the HSQC and HMBC spectra were treated as if they arose from two separate groups of structures and the ^{13}C shifts of the cross-peaks in the HSQC spectrum were correlated with cross-peaks in the HMBC spectrum having ^1H chemical shifts that could be attributed to EEBEE pentad structures.

The planes of 3D-HC_AC_X spectrum, parts b, c, and d of Figure 6 are taken at f_1 positions from the 3D spectrum corresponding to the chemical shifts of different peaks in the ester-carbonyl region of the 1D ^{13}C spectrum of polyEB*C at $\delta_{C=O} = 175.40$, 175.29, and 175.16 ppm, respectively. The cross-peaks, ***a***, ***b***, and ***c***, in the HC_AC_X spectrum, all appear at the same nominal ^1H shift of 2.35 ppm (consistent with that expected for CH_{EBE} protons), but they occur at different ^{13}C chemical shifts in both the f_1 and f_2 dimensions. The cross-peaks in these planes all correspond to those found in the poorly resolved A_1/A_2 cluster of peaks in the region of the HSQC spectrum shown in Figure 6a.

The cross-peaks in the HC_AC_X planes were assigned with the help of the HC_AC_X-$^1H^1H$-TOCSY spectrum, in the same way that short- and long-range correlations from HSQC, and HMBC or HSQC-TOCSY 2D-NMR spectra are used together to determine organic structures. Selected planes from the HC_AC_X-$^1H^1H$-TOCSY spectrum (Figure 6h−l) are shown below the planes from the HC_AC_X spectrum with the corresponding f_1 chemical shifts. Each plane in the HC_AC_X-$^1H^1H$-TOCSY spectrum shows the same HC_AC_X correlation (**a**, **b**, and **c**) that is observed in the corresponding plane of the HC_AC_X spectrum, and additional cross-peaks from $^1H^1H$-TOCSY transfer to neighboring protons. For example, in Figure 6h additional TOCSY cross-peaks $\mathbf{a}_1$ and $\mathbf{a}_{2/2'}$ are observed at $\delta_H = 1.32$, 1.44, and 1.67 ppm, which indicate that the center CH_B is present in a very symmetrical environment with same neighboring monomers on both sides. The cross-peak at $\delta_H = 1.32$ arises from $\beta^B\delta^+$ protons, while the nonequivalent $\alpha^B\delta^+$ methylene protons give rise to a pair of cross-peaks at $\delta_H = 1.44$ and 1.67 ppm. From these correlations it is obvious that the 3D-HC_AC_X cross-peaks ***a***, ***b***, and ***c*** arise from EBE triads present in highly symmetrical environments of EEBEE pentads. The variation of the environment around the pentads in higher *n*-ads accounts for the different ^{13}C chemical shifts of the cross-peaks. Based on the monomer composition (E:B:C = 66:4:30) of the polymer, these are most likely from EEEBEEE, CEEBEEE, and EEEBEEC heptads; however, the specific assignments for these higher *n*-ads cannot be made from the data available.

The other two broad overlapping cross-peaks (cluster B_1/B_2) in the HSQC spectrum (Figure 6a) are also spread in the f_1 dimension in the 3D-NMR spectra (Figure 6d,e), indicating that several peaks arising from higher *n*-ad environments are present and form the cluster in the 2D-NMR spectra. The f_1 planes of the 3D-HC_AC_X spectrum (Figure 6e,f) each correspond to a different peak in the ester-carbonyl region of the 1D ^{13}C spectrum from polyEB*C, at $\delta_{C=O} = 175.0$ and 174.83 ppm, respectively. The cross-peaks in the HC_AC_X spectra appear at a slightly different ^1H chemical shift of 2.38 ppm (cross-peaks ***d*** and ***e***) compared to those assigned above to EEBEE pentads. These cross-peaks also show slightly different ^{13}C chemical shift and were assigned with the help of the HC_AC_X-$^1H^1H$-TOCSY 3D-NMR spectrum. Cross-peaks ***d*** and ***e*** both show TOCSY correlations to proton resonances at $\delta_H = 1.32$ (cross-peaks ***d₁*** and ***e₁***), 1.44 (cross-peaks ***d₂*** and ***e₂***), and 1.66 ppm (cross-peaks ***d₂′*** and ***e₂′***) as were seen in the planes of EBE triads centered in EEBEE pentads in the discussion above. Therefore, these planes must arise from **B**-centered pentads within EE**B**XX or XX**B**EE units. Additional TOCSY correlations are observed to proton resonances at $\delta_H = 1.82$ (cross-peaks ***d₃*** and ***e₃***), 1.92 (cross-peaks ***d₃′*** and ***e₃′***), and 2.45 ppm (cross-peak ***d₄*** and ***e₄***) which indicate the presence of different neighboring monomer units on the opposite side of the central E**B**E triad. The pair of cross-peaks at $\delta_H = 1.82$ and 1.92 ppm are consistent with nonequivalent diastereotopic protons α to the CH branch point of the central B unit. The significant downfield shift of the resonances along ^1H dimension is attributed to the deshielding effect of a β-C unit. Therefore, these resonances are attributed to the nonequivalent $\alpha^B\beta^C$ protons. The cross-peaks at $\delta_H = 2.45$ ppm are consistent with the shift of methylene protons α to a carbonyl group and can be confidently attributed to $\alpha^C\beta^B$ protons. This indicates that EBE triad is present in EEBEC pentad which, in turn, is present in at least two higher *n*-ad environments as indicated by the two different ^{13}C shifts of the HC_AC_X cross-peaks. The low probability of B (ratio of E:C:B = 66:30:4) plus the improbability of C adding to C$^\bullet$ radical at the end of the polymer chain leads to the conclusion that these planes are from XEEBEC heptads, where X = E or C (in ca. 2:1 ratio of EEEBECE:CEEBECE if the polymerization were random). The concentration of BEEBECE is probably too low to detect (almost an order of magnitude lower than CEEBECE heptads if there is random polymerization). Since the structure fragments producing these correlations are similar (i.e., all EBE triads), they will have similar *J*-couplings and relaxation characteristics. Therefore, it should be reasonable to at least use relative cross-peak intensities as a basis of identifying at least which is the major component. Based on the number of contours, the intensity of cross-peak ***e*** is 2−3 times greater than cross-peak ***d***; therefore, these are tentatively assigned to EEEBECE and CEEBECE heptads, respectively.

CBE-Centered Structures. Figure 7 shows selected f_2f_3 planes ($^{13}C_{aliphatic}-^1H$ correlations) in the regions near $f_2 = 40.5$ ppm from the HC_AC_X (Figure 7b−e) and HC_AC_X-$^1H^1H$-TOCSY (Figure 7g−j) 3D-NMR spectra polyEB*C which arise from $^1H-^{13}C-^{13}C{=}O$ structure fragments along with the corresponding regions from the HSQC (Figure 7a) and HMBC (Figure 7f) 2D-NMR spectra of polyEB*^{2}C. The broad HSQC cross-peak (cluster ***C₁***) is dispersed into three different planes of the 3D-HC_AC_X spectrum. The f_1 planes of the HC_AC_X spectrum (Figure 7b−d) correspond to $\delta_{C=O} = 174.70$, 174.60, and 174.45 ppm, respectively. The cross-peaks in the HC_AC_X spectrum (cross-peaks ***f***, ***g***, and ***h***) all appear at an ^1H chemical shift of 2.91 ppm, indicating they all arise from similar triad sequences.

CDV

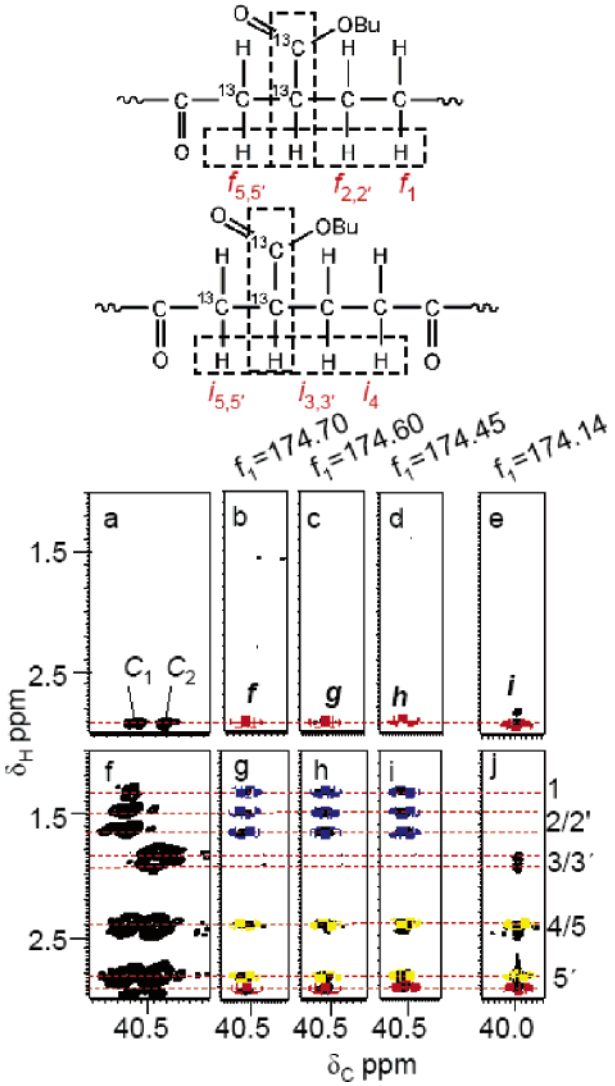

Figure 7. Expansions from the 2D- and 3D-NMR spectra of ^{13}C-labeled poly(EB*C) showing the 39.5−41.5 ppm region: (a) HSQC spectrum of polyEB*^{2}C; (b−e) f_2f_3 planes from the 3D-HC$_A$C$_X$ spectrum of polyEB*C; (f) HMBC spectrum of polyEB*^{2}C; (g−j) f_2f_3 planes from the 3D-HC$_A$C$_X$-^{1}H^{1}H-TOCSY spectrum of polyEB*C and assignment of ECBEE and ECBEC pentads. The f_1 chemical shifts are printed across the tops of the respective planes from the 3D spectra.

All these cross-peaks show HH-TOCSY correlations to a set of five additional proton resonances in the HC$_A$C$_X$-^{1}H^{1}H-TOCSY spectrum. The peaks at $\delta_H = 1.32$ (cross-peaks ***f*$_1$**, ***g*$_1$**, and ***h*$_1$**), 1.44 (cross-peaks ***f*$_2$**, ***g*$_2$**, and ***h*$_2$**), and 1.66 ppm (cross-peaks ***f*$_{2'}$**, ***g*$_{2'}$**, and ***h*$_{2'}$**) are readily identified from previous assignments as arising from $\beta^B\delta^+$ and nonequivalent $\alpha^B\delta^+$ protons, respectively, of **B**EE or EE**B** triads on either side of **B**-centered pentads. The TOCSY cross-peaks to the proton resonances $\delta_H \sim 2.43$ (cross-peaks ***f*$_5$**, ***g*$_5$**, and ***h*$_5$**) and 2.83 ppm (cross-peaks ***f*$_{5'}$**, ***g*$_{5'}$**, and ***h*$_{5'}$**) are identified as nonequivalent α^B protons; their downfield ^{1}H chemical shift indicates the presence of an attached C monomer unit. These cross-peaks are therefore attributed to the nonequivalent $\alpha^C\alpha^B$ protons of C**B** dyads. Consequently, the cross-peaks ***f***, ***g***, and ***h*** are assigned to the CBE triads present in XCBEE pentads, where X = E or B. The nature of X cannot be identified from correlations in the 3D spectra as proton TOCSY transfer is interrupted by the presence of C unit; however, X is unlikely to be C as CC dyads are not possible. From Table 3 it is seen that the ratio of the formation probabilities of ECBEE and BCBEE pentads is at least 8:1, from which it can be concluded that ECBEE pentads are far more likely to occur than BCBEE pentads; therefore, the cross-peaks primarily arise from ECBEE pentads. The different $^{13}C_\alpha$ shifts of cross-peaks ***f***, ***g***, and ***h*** indicate the presence of ECBEE pentads in higher *n*-ad environments. On the basis of the relative probabilities of E, C, and B monomers in the polymer, the three planes can be attributed to EECBEEE, CECBEEE, and EECBEEC heptads; however, the assignments specific heptads cannot be made with the present data.

The other broad cross-peak (cluster ***C*$_2$**) in the HSQC (Figure 7a) spectrum remains as a single set of cross-peaks in the 3D-HC$_A$C$_X$ spectrum (Figure 7e). This 3D-HC$_A$C$_X$ plane corresponds to $\delta_{C=O} = 174.14$ ppm. The cross-peak ***i*** appears at $\delta_H = 2.92$ ppm and is correlated to four additional proton chemical shifts in the HC$_A$C$_X$-^{1}H^{1}H-TOCSY spectrum. The cross-peaks at $\delta_H = 1.82$ (cross-peak ***i*$_3$**), 1.92 (cross-peak ***i*$_{3'}$**), and 2.43 ppm (cross-peak ***i*$_4$**) are at the same ^{1}H chemical shifts that were previously attributed to nonequivalent $\alpha^B\beta^C$ (δ_H = 1.82 and 1.92 ppm) and $\alpha^C\beta^B$ ($\delta_H = 2.40$ ppm) protons of **B**EC triads (see prior section). The nonequivalent $\alpha^C\alpha^B$ protons of XC**B** triads produce cross-peaks ***i*$_5$** and ***i*$_{5'}$** (δ_H = 2.43 and 2.83 ppm). One of the resonances of the nonequivalent $\alpha^C\alpha^B$ protons overlaps with $\alpha^C\beta^B$ proton resonance at $\delta_H \sim 2.45$ ppm.

These cross-peaks indicate the presence of CBE-centered XC**B**EC pentads, where X = E or B. The nature of X cannot be confirmed as proton TOCSY transfer is inhibited by the presence of C unit in the XC**B** triad of XC**B**EC pentad. But the statistical formation probability of ECB triads is ca. 8 times higher than that of BCB triads as seen from the calculated Bernoullian distribution of sequences in Table 3. Therefore, it is probable that the C**B**E triads are predominantly present in EC**B**EC pentads.

BBE-Centered Structures. Figure 8 shows selected f_2f_3 planes ($^{13}C_{aliphatic}$−^{1}H correlations) from the HC$_A$C$_X$ (Figure 8b−f) and HC$_A$C$_X$-^{1}H^{1}H-TOCSY (Figure 8h−l) 3D-NMR spectra of polyEB*C, which arise from ^{1}H−^{13}C−^{13}C═O structure fragments, along with the corresponding regions from the HSQC (Figure 8a) and HMBC (Figure 8g) 2D-NMR spectra of polyEB*^{2}C. Three different clusters of cross-peaks (***D*$_1$**, ***D*$_2$**, and ***D*$_3$**) consisting of at least a dozen poorly resolved, low-intensity cross-peaks are observed in this area of the 2D-NMR spectra, indicating the complexity of the mixture of structures containing BB dyads. In the 3D-HC$_A$C$_X$ spectrum, these resonances are dispersed into 16 different planes, each separated by ca. 0.03 ppm along the f_1 (ester carbonyl ^{13}C chemical shift) dimension. Five representative f_1 planes are shown from the HC$_A$C$_X$ 3D-spectrum (Figure 8b−f), corresponding to $\delta_{C=O}$ = 175.03, 174.94, 174.84, 174.65, and 174.55 ppm, respectively. None of these are adjoining planes, and they are typically separated by two or three planes. The cross-peaks (***j***, ***k***, ***l***, ***m***, and ***n***) in the HC$_A$C$_X$ spectra appear at $\delta_H \sim 2.50$ ppm, indicating they all arise from similar triad sequences. The ^{13}C shifts of the cross-peaks in the f_2 (aliphatic carbon chemical shift region) dimension move progressively upfield along with the shift in the f_1 (carbonyl region) dimension.

These (***j***, ***k***, ***l***, ***m***, and ***n***) HC$_A$C$_X$ cross-peaks are related to TOCSY correlations with a number of proton resonances in the f_3 dimension. The TOCSY cross-peaks appear at δ_H = 1.33, 1.48, 1.66, 1.84, 1.85, 1.93, 2.15, 2.46, and 2.58 ppm. HC$_A$C$_X$ cross-peak ***j*** shows correlations to six TOCSY cross-peaks ***j*$_1$**, ***j*$_{2/2'}$**, ***j*$_6$**, and ***j*$_{8'}$**. (The weak cross-peak at ***j*$_{7'}$** is bleed-through from an adjoining slice.) The cross-peaks ***j*$_1$** and ***j*$_{2/2'}$** can readily be assigned to $\beta^B\delta^+$ and nonequivalent $\alpha^B\delta^+$ protons, respectively, of **B**EE sequences, based on previous assignments of ^{1}H

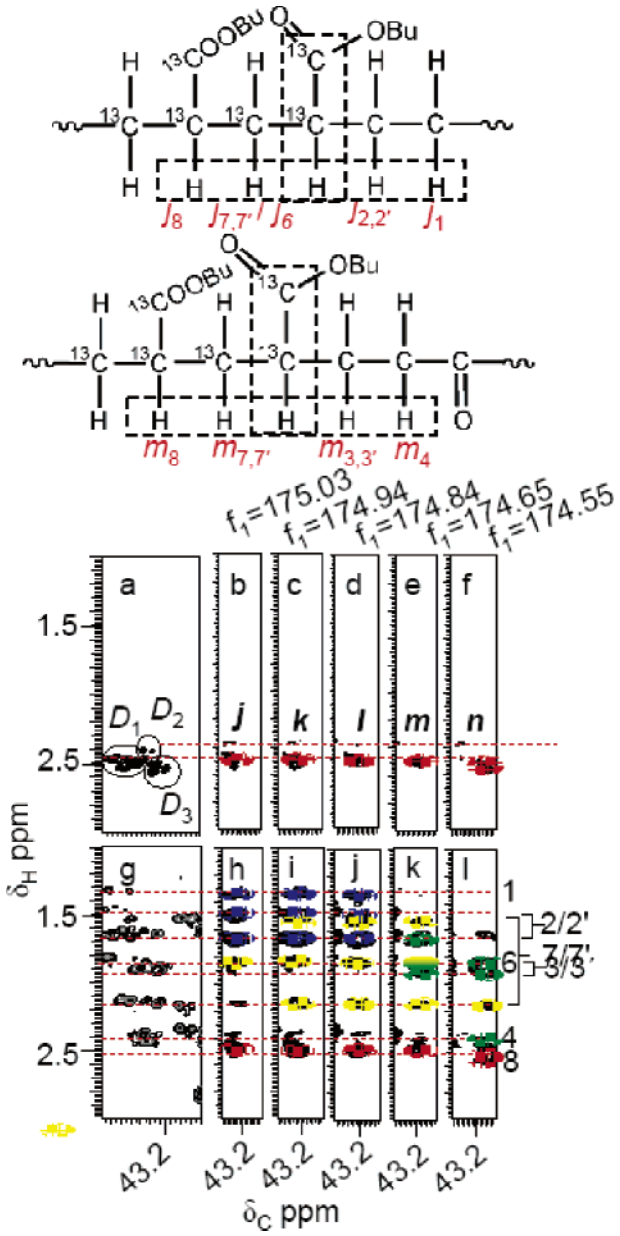

Figure 8. Expansions from the 2D- and 3D-NMR spectra of ^{13}C-labeled poly(EB*C) showing the 42.5−44.5 ppm region: (a) HSQC spectrum of polyEB*^{2}C; (b−f) f_2f_3 planes from the 3D-HC_AC_X spectrum of polyEB*C; (g) HMBC spectrum of polyEB*^{2}C; (h−l) f_2f_3 planes from the 3D-HC_AC_X-$^{1}H^{1}$H-TOCSY spectrum of polyEB*C, along with labels showing the assignment of specific cross-peaks to H−C correlations in EBBEE and EBBEC pentad structures.

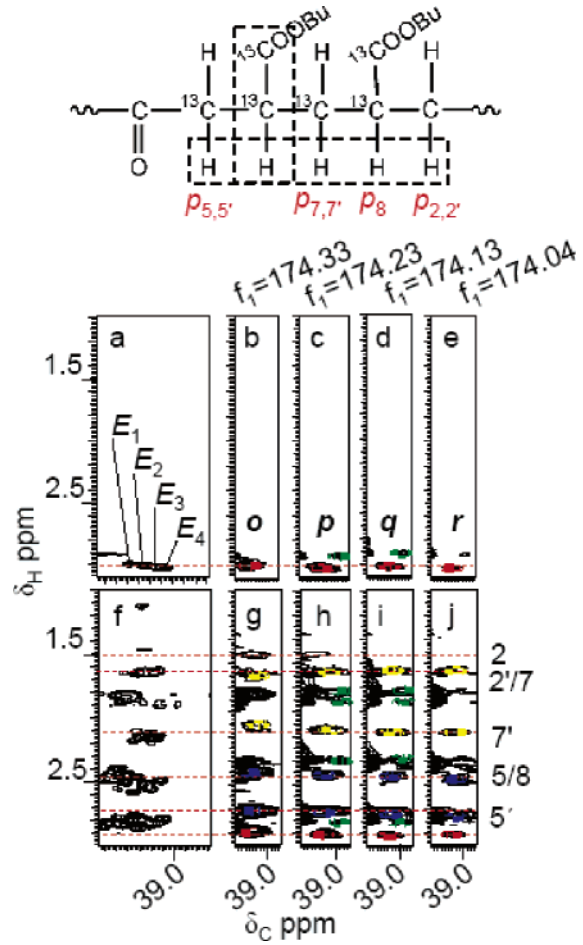

Figure 9. Expansions from the 2D- and 3D-NMR spectra of ^{13}C-labeled poly(EB*C) showing the 38.5−39.5 ppm region: (a) HSQC spectrum of polyEB*^{2}C; (b−e) f_2f_3 planes from the 3D-HC_AC_X spectrum of polyEB*C; (f) HMBC spectrum of polyEB*^{2}C; (g−j) f_2f_3 planes from the 3D-HC_AC_X-$^{1}H^{1}$H-TOCSY spectrum of polyEB*C and assignment of C**B**B triad.

chemical shifts. This indicates the presence of the B**B**E triad in XB**B**EE pentads. The ***j*$_6$** and ***j*$_8$** cross-peaks are attributed to equivalent $\alpha^B\alpha^B$ protons of *racemic* B**B** dyads and the CH_{BBE} of B**B**E triad, respectively. HC_AC_X cross-peaks ***k*** and ***l*** show an additional TOCSY correlation to proton resonances at δ_H = 2.15 ppm (cross-peaks ***k*$_{7'}$** and ***l*$_{7'}$**). The cross-peaks at these proton shifts are identified from the 2D-NMR data of poly(ethylene-*co*-*n*-butyl acrylate)[39] as arising from one of the nonequivalent $\alpha^B\alpha^B$ protons of *meso*-BB dyads. The resonance from the second diastereotopic $\alpha^B\alpha^B$ proton occurs at δ_H = 1.66 and overlaps with one of the $\alpha^B\delta^+$ correlations denoted 7 on the figure. Cross-peaks ***k*** and ***l*** are therefore attributed to BBE triads containing *meso*-BB dyads (i.e., (EEBmBX pentads where X = E or B). More definitive assignments are not possible with the data in hand.

Cross-peaks ***m*** and ***n*** are related to TOCSY cross-peaks at δ_H = 1.44, 1.66, 1.82, 1.92, 2.15, 2.4, and 2.46 ppm. The pair of cross-peaks (***m*$_{3/3'}$** and ***n*$_{3/3'}$**) at δ_H = 1.82 and 1.92 were previously attributed to nonequivalent $\alpha^B\beta^C$ protons. This indicates the presence of a C unit next to BBE triad. The cross-peaks ***m*** and ***n*** are attributed to B**B**E triads present in EB**B**EC and CE**B**BE pentads.

Thus, we can conclude that B**B**E triads, responsible for the planes in Figure 8, are present in two different types of pentad monomer sequences, XB**B**EE and XB**B**EC, with B**B** dyad in both the *meso* and *racemic* forms. The X in the pentad sequences can be E, B, or C. However, the shift of the TOCSY cross-peak m_8 proves that X cannot be C. The ratio of the formation probabilities of EB**B**, BB**B**, and CB**B** triads is 8:1:3, based on a Bernoullian distribution. This indicates that EB**B** is more likely to occur compared to the other two triads and BBE triads are predominantly present in EBBEE and EBBEC pentads.

CBB-Centered Structures. Figure 9 shows selected f_2f_3 planes ($^{13}C_{aliphatic}$−^{1}H correlations) from HC_AC_X (Figure 9b−e) and HC_AC_X-$^{1}H^{1}$H-TOCSY (Figure 9g−j) 3D-NMR of polyEB*C spectra which arise from ^{1}H−^{13}C−^{13}C═O structure fragments in CBB triads, along with the corresponding regions from the HSQC (Figure 9a) and HMBC (Figure 9f) 2D-NMR spectra of polyEB*^{2}C. The four overlapping HSQC cross-peaks (***E*$_1$**, ***E*$_2$**, ***E*$_3$**, and ***E*$_4$**) are dispersed into four different planes along the f_1 dimension of the 3D-HC_AC_X spectrum. The f_1 planes

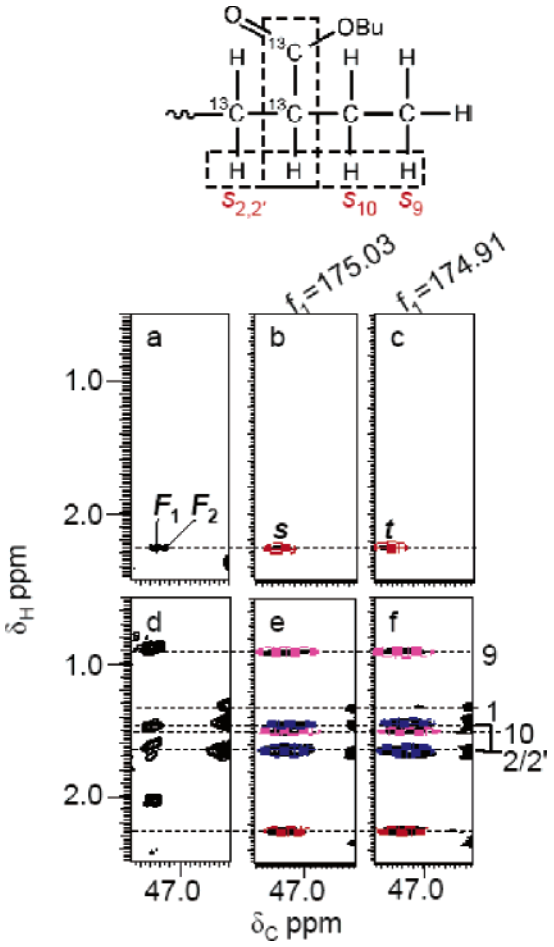

Figure 10. Expansions from the 2D- and 3D-NMR spectra of labeled poly(EB*C) showing the 46.0−48.0 ppm region: (a) HSQC spectrum of polyEB*^{2}C; (b−c) f_2f_3 planes from the 3D-HC$_A$C$_X$ spectrum of polyEB*C; (d) HMBC spectrum of polyEB*^{2}C; (e, f) f_2f_3 planes from the 3D-HC$_A$C$_X$-^{1}H^{1}H-TOCSY spectrum of polyEB*C; along with assignments labeled on the structure of an −∼EEBE chain-end structure.

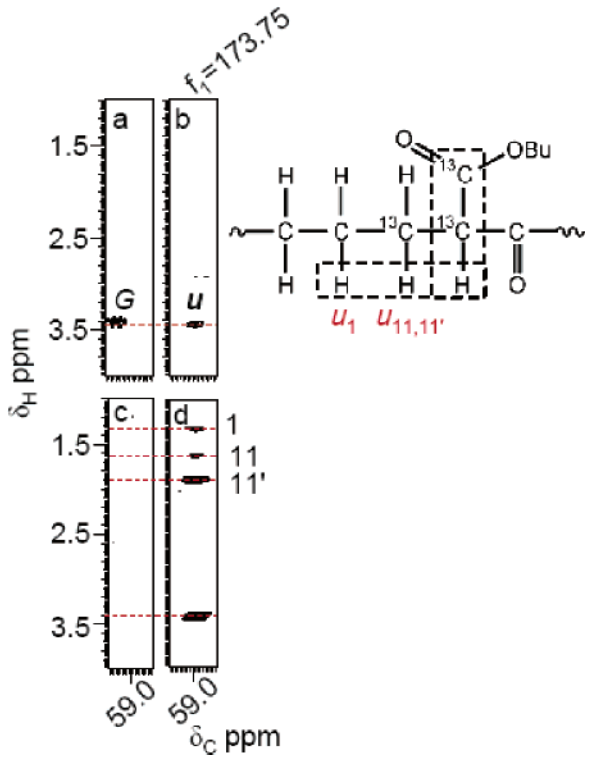

Figure 11. Expansions from the 2D- and 3D-NMR spectra of labeled poly(EB*C) showing the 58.0−60.0 ppm region: (a) HSQC spectrum of polyEB*^{2}C; (b) f_2f_3 plane from the 3D-HC$_A$C$_X$ spectrum of polyEB*C; (c) HMBC spectrum of polyEB*^{2}C; (d) f_2f_3 plane from the 3D-HC$_A$C$_X$-^{1}H^{1}H-TOCSY spectrum of polyEB*C and assignment of BC dyad.

of the HC$_A$C$_X$ spectrum in Figure 9b−e correspond to $\delta_{C=O}$ = 174.33, 174.23, 174.13, and 174.04 ppm, respectively. The cross-peaks ***o***, ***p***, ***q***, and ***r*** in the HC$_A$C$_X$ spectra all appear at $\delta_H \sim$ 2.92 ppm, indicating they all arise from similar triad sequences. The large downfield ^{1}H chemical shift of these CH cross-peaks is consistent with proton resonances of CH$_B$ groups which are β to the ketone carbonyl groups of C units of C**B** dyads in the polymer backbone. These HC$_A$C$_X$ cross-peaks are each related to six TOCSY cross-peaks in the 3D HC$_A$C$_X$-^{1}H^{1}H-TOCSY spectrum. The proton chemical shifts of these TOCSY cross-peaks have already been assigned in the previous sections. The TOCSY cross-peaks to proton resonances at δ_H = 2.43 (cross-peaks o_5, p_5, q_5, and r_5) and 2.83 ppm (cross-peaks $o_{5'}$, $p_{5'}$ $q_{5'}$, and $r_{5'}$) are attributed to nonequivalent $\alpha^C\alpha^B$ protons of XC**B** triads. The TOCSY cross-peak to proton resonances near δ_H = 1.66 and 2.15 (cross-peaks $o_{7/7'}$, $p_{7/7'}$ $q_{7/7'}$, and $r_{7/7'}$) are attributed to the nonequivalent $\alpha^B\alpha^B$ protons of the **B**B dyad. Many of the other weak cross-peaks, such as o2 and p2, and the series of cross-peasks at ca. δ_H = 1.8 ppm are likely to be bleed-through from adjoining downfield slices which result from resonances that are an order of magnitude greater than those producing cross-peaks attributed to these planes. While planes from four separate CBB-containing structures (from pentad monomer- or stereosequence effects) are clearly resolved, it is not possible to reliably assign these planes to specific pentad structures on the basis of data in hand.

Other Structures. Figure 10 shows selected f_2f_3 planes (^{13}C$_{aliphatic}$−^{1}H correlations) from HC$_A$C$_X$ (Figure 10b,c) and HC$_A$C$_X$-^{1}H^{1}H-TOCSY (Figure 10e,f) 3D-NMR spectra of labeled polyEB*C along with the HSQC (Figure 10a) and HMBC (Figure 10d) 2D-NMR spectra of polyEB*^{2}C. The cross-peaks ***s*** and ***t*** appear at δ_H = 2.25 ppm (at very different shifts from the corresponding correlations of EE**B** structures discussed in association with the data presented in Figure 6 above) and show TOCSY correlations to the shifts of four proton resonances in the HC$_A$C$_X$-^{1}H^{1}H-TOCSY spectrum. Among them, cross-peaks at $s_{2/2'}$ and $t_{2/2'}$ have previously been identified as nonequivalent $\alpha^B\delta^+$ protons; traces of signals that might be attributed to weak cross-peaks (s_1 and t_1) from $\beta^B\delta^+$ protons are also observed. Additional TOCSY cross-peaks to proton resonances at δ_H = 0.9 and 1.50 ppm (s_9/s_{10} and t_9/t_{10}) are attributed to the methyl and methylene protons of an ethyl group attached to the −EE**B** structure, indicating that these planes arise from chain-end structures ∼EEBE present in two different environments as ***s*** and ***t*** differ in their chemical shifts along ^{13}C$_{aliphatic}$ dimension.

Figure 11 shows selected f_2f_3 planes (^{13}C$_{aliphatic}$−^{1}H correlations) from HC$_A$C$_X$ (Figure 11b) and HC$_A$C$_X$-^{1}H^{1}H-TOCSY (Figure 11d) 3D-NMR spectra of polyEB*C which arise from ^{1}H−^{13}C−^{13}C=O structure fragments, along with the corresponding regions from HSQC (Figure 11a) and HMBC (Figure 11c) 2D-NMR spectra of polyEB*^{2}C. The f_1 plane of the HC$_A$C$_X$ spectrum corresponds to $\delta_{C=O}$ = 173.75 ppm. The cross-peak, u, appears at δ_H = 3.44 ppm and shows TOCSY correlations to the resonances of three protons at δ_H = 1.32, 1.63, and 1.90 ppm. The large downfield ^{1}H chemical shift of cross-peak ***u*** indicates that this methine proton has a neighboring C unit. This indicates the presence of a BC dyad, formation of which was ruled out earlier because of unfavorable steric/electronic con-

siderations. To confirm the assignment of these correlations to BC dyads, a model compound, **7**, was prepared and the ^{13}C

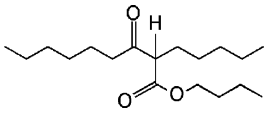

7

and ^{1}H chemical shifts of its CH_B resonances were compared with those of the 3D-NMR correlations attributed to BC dyads. The cross-peaks at $\delta_H = 1.32$ (cross-peak u_1) were previously identified as $\beta^B\delta^+$ protons. The other two cross-peaks, $u_{11/11'}$, are assigned with the help of the model compound and identified as nonequivalent $\alpha^B\delta^+$ protons of B units bound to a ketone carbonyl. However, this peak indicates that BC dyads form in the random polymerization even though they are present to a very small extent. Remember that ^{13}C labeling was necessary to enhance these signals 100-fold for detection and that these are proton-detected experiments. It is not possible to detect these signals in a standard 1D proton spectrum collected in a relatively short period of time, since it took many hours to collect the 3D data set which has 1−2 orders of magnitude better signal-to-noise.

3D-NMR of Singly ^{13}C-Labeled Polymers. The 3D-HC_AC_X and HC_AC_X-$^1H^1H$-TOCSY spectra were also collected with the samples of polyEB*^{1}C and polyEB*^{2}C and processed in the same manner. Similar results were obtained in each case, but only signals from pentad structures with high probability of occurrence can be detected. Resonances from triads having BB dyads cannot be detected in these 3D spectra because of their weak signal intensity. All the TOCSY correlations observed in the 3D spectra of polyEB*C are also observed in these spectra.

Comparison of 2D- and 3D-NMR Spectra. Monwar et al.[22] used 2D-NMR studies of labeled polyEB*^{1}C and polyEB*^{2}C and were able to get complete assignments for the ^1H and ^{13}C resonances of six pentad structures and partial assignments for four other structures with the help of HSQC and HMBC 2D-NMR spectra. Although they were successful in assigning a number of resonances, in some cases the assignments were ambiguous. They found it particularly difficult to resolve resonances in the regions of 42.5−44.5 and 38.5−39.5 ppm, where the resonances from BBE and CBB triads occur. These are low occurring triads and exhibit very weak, overlapping HMBC cross-peaks. In 3D-NMR these overlapped peaks are dispersed into a third dimension ($\delta_{C=O}$). Moreover, the broad peaks of 2D spectra are narrowed and show sharp cross-peaks as $^{13}C-^{13}C$ coupling is effectively removed in 3D-NMR, while the uniform labeling eliminates the problem of sensitivity. Sharp, strong, and well-resolved cross-peaks help in unambiguous assignment, and peaks are identified and assigned with ease. In addition to these advantages, the 3D-NMR spectra show new correlations and structures which reveal much more information about the structure of the polymer.

Conclusion

The complex problem of characterizing hydrocarbon-based polymer structures and assigning their NMR resonances can be solved with greater ease and less ambiguity using 3D-NMR, selective ^{13}C-labeling, and use of shaped pulses which treat the resolved resonances from one set of ^{13}C atoms in the structure as the third nuclei. The use of a high field spectrometer provides higher sensitivity and well-resolved peaks which, when combined with atomic connectivity information provided by 3D-NMR, greatly simplifies the complex spectra and ensures the unambiguous assignment of the resonances arising from different monomer *n*-ads, branching structures, and chain-ends. In particular, the methodology permitted the resolution and identification of low-concentration structures such as BC dyads and chain-end resonances that were previously undetectable or not thought to exist. The identification of the structures present in this complex polymer and assignment of their resonances will be useful for understanding the mechanisms of the reactions controlling polymerization and for characterizing structure−property relationships in this important commercial material. These techniques are more general than those previously used and can be applied to study the structures of other complex polymers and mixtures of small molecules.

Acknowledgment. The authors acknowledge the National Science Foundation (DMR-0073346 and DMR-0324964) and E.I. du Pont de Nemours and Co. for support of this research and the Kresge Foundation and donors to the Kresge Challenge program at the University of Akron for funds used to purchase the 750 MHz NMR instrument used for this work. The authors also thank Drs. Michael M. Buback and Henning Latz for making the ^{13}C-labeled polymers. Thanks are due to V. Dudipala, J. Massey, and S. Stakleff for their support in maintaining the NMR facilities used in this work.

Supporting Information Available: High-resolution PDF files containing the data presented in the figures so that the raw data are available for scrutiny that would not be possible by examining the spectra presented in the printed version of the paper; 1D- and 2D-NMR spectra of model compound **7**; 2D-NMR spectra (HSQC and HMBC) of singly labeled poly(EB*^{1}C) and 3D-HC_AC_X and 3D-HC_AC_X-TOCSY spectra of singly labeled poly(EB*^{1}C) and poly(EB*^{2}C); and complete analysis of 1D and 2D (HSQC and HMBC) spectra of poly(ethylene-*co*-*n*-butyl acrylate) samples. This material is available free of charge via the Internet at http://pubs.acs.org.

References and Notes

(1) Randall, J. C. *J. Macromol. Sci., Rev. Macromol. Chem. Phys.* **1989**, *C29*, 201.
(2) Bruch, M. D.; Payne, W. G. *Macromolecules* **1986**, *19*, 2712.
(3) Liu, W.; Ray, D. G., III.; Rinaldi, P. L.; Zens, T. *J. Magn. Reson.* **1999**, *140*, 482.
(4) Liu, W.; Rinaldi, P. L.; McIntosh, L. H.; Quirk, R. *P. Polym. Prepr. (Am. Chem. Soc., Div. Polym. Chem.)* **2000**, *41*, 30.
(5) Sahoo, S. K.; Zhang, T.; Dudipala, V. R.; Rinaldi, P. L.; McIntosh, L. H.; Quirk, R. P. *Macromolecules* **2003**, *36*, 4017.
(6) McCord, E. F.; Shaw, W. H., Jr.; Hutchinson, R. A. *Macromolecules* **1997**, *30*, 246.
(7) Rinaldi, P. L. In *NMR Spectroscopy of Polymers in Solution and in the Solid State*; Cheng, H. N., English, A. D., Eds.; ACS Symposium Series 834; American Chemical Society: Washington, DC, 2003; Chapter 8, p 94.
(8) Rinaldi, P. L. *Analyst* **2004**, *129*, 687.
(9) Rinaldi, P. L.; Ray, D. G., III; Li, L.; Wang, H. T.; Harwood, H. J. *Multidimensional Spectroscopy of Polymers*; Urban, M. W., Provder, T., Eds.; ACS Symposium Series 598; American Chemical Society: Washington, DC, 1995; Chapter 13.
(10) Li, L.; Ray, D.; Wang, H. T.; Harwood, H. J.; Rinaldi, P. L. *Macromolecules* **1996**, *29*, 4706.
(11) Rinaldi, P. L.; Ray, D. G., III; Li, L.; Wang, H. T.; Harwood, H. J. *Polym. Mater. Sci. Eng.* **1994**, *71*, 269.
(12) Li, L.; Rinaldi, P. L. *Macromolecules* **1996**, *29*, 4808.
(13) Li, L.; Rinaldi, P. L. *Macromolecules* **1997**, *30*, 520.
(14) Saito, T.; Medsker, R. E.; Harwood, H. J.; Rinaldi, P. L. *J. Magn. Reson. A* **1996**, *120*, 125.
(15) Liu, W.; Saito, T.; Li, L.; Rinaldi, P. L.; Hirst, R.; Halasa, A. F.; Visintainer, J. *Macromolecules* **2000**, *33*, 2364.
(16) Liu, W.; Rinaldi, P. L.; Galya, L.; Hansen, J. E.; Wilczek, L. *Organometallics* **2002**, *21*, 3250.
(17) Chai, M.; Tessier, C.; Rinaldi, P. L. *J. Am. Chem. Soc.* **1999**, *121*, 273.

(18) Sahoo, S. K.; McCord, E. F.; Rinaldi, P. L. *J. Magn. Reson.* **2004**, *168*, 352.
(19) Patt, S. L. *J. Magn. Reson.* **1992**, *96*, 94.
(20) Note that *n*-ad sequences in vinyl polymers normally are structurally indistinguishable if the order of monomer addition is reversed; however, this is not the case with these polymers containing units from carbon monoxide, which contributes only one carbon to the polymer backbone.
(21) Wyzgoski, F. J.; Rinaldi, P. L.; McCord, E. F.; Stewart, M. A.; Marshall, D. R. *Macromolecules* **2004**, *37*, 846.
(22) Monwar, M.; Oh, S. J.; Rinaldi, P. L.; McCord, E. F.; Hutchinson, R. A.; Buback, M. M.; Latz, H. *J. Anal. Bioanal. Chem.* **2004**, *378*, 1414**.**
(23) Al-Amri, A.; Monwar, M.; McCord, E. F.; Buback, M.; Latz, H.; Rinaldi, P. L. *Macromolecules*, submitted for publication.
(24) Bodenhausen, G.; Ruben, D. J. *Chem. Phys. Lett.* **1980**, *69*, 565.
(25) Bax, A.; Summers, M. F. *J. Am. Chem. Soc.* **1986**, *108*, 2093.
(26) Shaka, A. J.; Barker, P. B.; Freeman, R. *J. Magn. Reson.* **1985**, *64*, 547.
(27) States, D. J.; Haberkorn, R. A.; Ruben, D. J. *J. Magn. Reson.* **1985**, *64*, 547.
(28) Monwar, M.; Sahoo, S. K.; Rinaldi, P. L.; McCord, E. F.; Marshall, D. R.; Buback, M.; Latz, H. *Macromolecules* **2003**, *36*, 6695.
(29) Marion, D.; Ikura, M.; Tschudin, R.; Bax, A. *J. Magn. Reson.* **1989**, *85*, 393.
(30) Kay, L. E.; Keiffer, P.; Saarinen, T. *J. Am. Chem. Soc.* **1992**, *114*, 10663.
(31) Xia, Y.; Kong, X.; Smith, D. K.; Liu, Y.; Man, D.; Zhu, G. *J. Magn. Reson.* **2000**, *143*, 407.
(32) Shaka, A. J.; Lee, C. J.; Pines, A. *J. Magn. Reson.* **1988**, *77*, 274.
(33) The Bernoullian probabilities are listed only as a rough guide to qualitatively describe the relative amounts of pentads; it is not meant to imply that the reactivities of the three monomers are equal.
(34) Carman, C. J.; Wilkes, C. E. *Rubber Chem. Technol.* **1971**, *44*, 781.
(35) Dorman, D. E.; Otocka, E. P.; Bovey, F. A. *Macromolecules* **1972**, *5*, 574.
(36) In this case, the term "branch" is used loosely, and the branch unit is formed by the replacement of the backbone methylene hydrogens with an oxygen atom.
(37) Morris, G. A.; Freeman, R. *J. Am. Chem. Soc.* **1979**, *101*, 760.
(38) Rama Krishna, N.; Berliner, L. J. *Protein NMR for the Millennium. Biological Magnetic Resonance*; Kluwer Academic/Plenum Publishers: New York, 2003; Vol. 20.
(39) See Supporting Information.

MA052572F